WL-TR-94-4046

LIFE PREDICTION METHODOLOGY FOR COMPOSITE LAMINATES

PART I: CONSTANT AMPLITUDE AND TWO-STRESS LEVEL FATIGUE

JEFFERY R. SCHAFF

BARRY D. DAVIDSON
DEPT OF MECHANICAL, AEROSPACE, AND MANUFACTURING ENGINEERING
SYRACUSE UNIVERSITY
SYRACUSE NEW YORK

SEPTEMBER 1994
INTERIM REPORT FOR 15 JAN 93 - 30 AUG 94

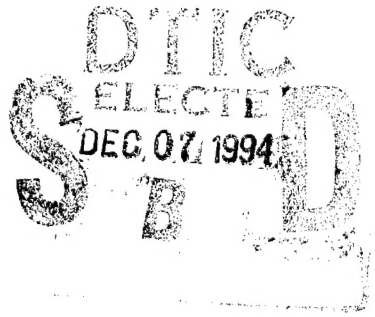

MATERIALS DIRECTORATE
WRIGHT LABORATORY
AIR FORCE MATERIEL COMMAND
WRIGHT PATTERSON AFB OH 45433-7734

NOTICE

When Government drawings, specifications, or other data are used for any purpose other than in connection with a definitely Government-related procurement, the United States Government incurs no responsibility or any obligation whatsoever. The fact that the government may have formulated or in any way supplied the said drawings, specifications, or other data, is not to be regarded by implication, or otherwise in any manner construed, as licensing the holder, or any other person or corporation; or as conveying any rights or permission to manufacture, use, or sell any patented invention that may in any way be related thereto.

This report is releasable to the National Technical Information Service (NTIS). At NTIS, it will be available to the general public, including foreign nations.

This technical report has been reviewed and is approved for publication.

Jeffery R. Schaff

JEFFERY R. SCHAFF, 1Lt, USAF
Materials Research Engineer
Mechanics & Surface Interactions Br

Wayne E. Ward

WAYNE E. WARD, Acting Chief
Mechanics & Surface Interactions Br
Nonmetallic Materials Division

George F. Schmitt

GEORGE F. SCHMITT
Assistant Chief
Nonmetallic Materials Division
Materials Directorate

If your address has changed, if you wish to be removed from our mailing list, or if the addressee is no longer employed by your organization please notify WL/MLBM , WPAFB, OH 45433-7750 to help us maintain a current mailing list.

Copies of this report should not be returned unless return is required by security considerations, contractual obligations, or notice on a specific document.

REPORT DOCUMENTATION PAGE

Form Approved
OMB No. 0704-0188

1. AGENCY USE ONLY (Leave blank)	2. REPORT DATE	3. REPORT TYPE AND DATES COVERED
	Sep 1994	INTERIM 15 Jan 93 - 30 Aug 94

4. TITLE AND SUBTITLE
LIFE PREDICTION METHODOLOGY FOR COMPOSITE LAMINATES
PART I: CONSTANT AMPLITUDE AND TWO-STRESS LEVEL FATIGUE

5. FUNDING NUMBERS

C - - -
PE 62102
PR 2419
TA 03
WU 10

6. AUTHOR(S)

JEFFERY R. SCHAFF
BARRY D. DAVIDSON

7. PERFORMING ORGANIZATION NAME(S) AND ADDRESS(ES)

MATERIALS DIRECTORATE
WRIGHT LABORATORY
AIR FORCE MATERIEL COMMAND
WRIGHT PATTERSON AFB OH 45433-7734

8. PERFORMING ORGANIZATION REPORT NUMBER

9. SPONSORING/MONITORING AGENCY NAME(S) AND ADDRESS(ES)

MATERIALS DIRECTORATE
WRIGHT LABORATORY
AIR FORCE MATERIEL COMMAND
WRIGHT PATTERSON AFB OH 45433-7734

10. SPONSORING/MONITORING AGENCY REPORT NUMBER

WL-TR-94-4046

11. SUPPLEMENTARY NOTES

12a. DISTRIBUTION/AVAILABILITY STATEMENT

APPROVED FOR PUBLIC RELEASE; DISTRIBUTION IS UNLIMITED.

12b. DISTRIBUTION CODE

13. ABSTRACT (Maximum 200 words)

A strength-based wearout model is presented for predicting the residual strength and life of composite laminates subjected to constant amplitude or two-stress level fatigue loadings. It is assumed that the laminate undergoes proportional loading, that its residual strength is a monotonically decreasing function of the number of loading cycles, and that the probability of failure after an arbitrary number of cycles may be represented by a two parameter Weibull function. The model also incorporates a "cycle mix factor" to account for the degradation of strength and life that may be associated with frequent changes in the stress amplitude of the loading. Experimental results from two-stress level loadings are used to evaluate the model's predictive capability for sequencing effects, as in a low-high or high-low test, and for cycle mix effects, as in a low-high-low-high repeating test. Good correlation between theory and experiment is obtained for all loadings and laminates studied.

14. SUBJECT TERMS

LIFE PREDICTION, FATIGUE, COMPOSITE MATERIALS

15. NUMBER OF PAGES
44

16. PRICE CODE

17. SECURITY CLASSIFICATION OF REPORT	18. SECURITY CLASSIFICATION OF THIS PAGE	19. SECURITY CLASSIFICATION OF ABSTRACT	20. LIMITATION OF ABSTRACT
UNCLASSIFIED	UNCLASSIFIED	UNCLASSIFIED	UL

TABLE OF CONTENTS

LIST OF FIGURES

1. INTRODUCTION

As a result of their high specific stiffness and specific strength, continuous fiber composites are often selected for weight-critical structural applications. However, deficiencies in current life prediction methodologies for these materials often force large factors of safety to be adopted. That is, composite structures used in high cycle fatigue applications are often "overdesigned" and are therefore somewhat heavier and more costly than necessary. Better life prediction methodologies may result in more efficient use of these materials and may result in lower weight and lower cost structures. For traditional aerospace applications, this has the added benefit of improved vehicle performance; it may also increase the attractiveness of composites for non-traditional applications.

A large number of models have been proposed to predict the residual strength and life of fatigue loaded composite structures. These models may be broadly characterized as either mechanistic or phenomenological. Mechanistic models, which we define as those which quantitatively account for the progression of damage in composite laminates, offer the long term promise to be applicable to a wide variety of materials, layups and loadings with a minimal amount of experimentally obtained input. At present, however, these models are either in their infancy or have only been applied to simple fatigue loadings (e.g., McLaughlin et al., 1975; Kulkarni et al., 1976; Talreja, 1985; Timmer and Hahn, 1993). Phenomenological models, which we define as those which characterize residual strength and life in terms of macroscopically observable properties, such as strength or stiffness, perhaps offer the most promising *near term* approach. The primary drawback of current phenomenological approaches is their dependency on large amounts of experimental input for each material, layup, and loading of interest.

In this two-part work, a new phenomenological model is developed for predicting the residual strength and life of fatigue loaded composite laminates. As in previous approaches, the model is semi-empirical; however, only a limited amount of experimental input is required for this model's characterization. Moreover, it will be shown that the model has very good predictive capability for both simple and complex load histories. Part I of this work considers the development and verification of the model for constant amplitude and two-stress amplitude fatigue. The model is validated for sequencing effects by comparing theoretical fatigue life predictions to experimental results for low-high and high-low two-stress amplitude test data. The model is also evaluated for its ability to predict the degradation of strength and life that may be caused by frequent changes in the stress amplitude of the loading. This

is accomplished by comparing predicted to experimental results for two-stress level low-high-low-high repeating tests with various load block sizes. Part II of this work (Schaff and Davidson, 1994b) considers extension of the model to a randomly ordered load spectrum.

2. PHENOMENOLOGICAL FATIGUE MODELS

In this section, a brief review of previous phenomenological fatigue models is presented. This review in *not* intended to be exhaustive, but rather to frame the motivation for the succeeding modelling approach. More extensive reviews can be found in Hwang and Han (1986a) or Sendeckyj (1991).

Previous phenomenological approaches to modelling fatigue failures of composite laminates can be broadly characterized as stiffness-based or strength-based. As the names imply, stiffness-based models utilize some measure of the laminate's stiffness as the primary variable upon which the model is based, whereas strength-based models utilize various measures of strength and stress. Either approach may be either deterministic, in which a single-valued life and/or residual strength are predicted, or statistical, in which predictions are for life and/or strength distributions.

The primary difficulty with stiffness-based models has been the development of a generally applicable failure criterion. Different failure criteria fundamentally based upon secant modulus (Hahn and Kim, 1976; O'Brien and Reifsnider, 1981; Whitworth, 1990, 1987; Farrow, 1989) and static strain-to-failure (Hwang and Han, 1986a, 1986b, 1989; Poursartip, Ashby, and Beaumont, 1986; Poursartip and Beaumont, 1986; Yang, Yang and Jones, 1989; Lee, Yang and Sheu, 1992) have been proposed. These criteria and their associated stiffness-based models have been used to obtain reasonable fatigue life predictions for constant amplitude and two-stress amplitude loadings. However, none of the approaches have been successfully applied to a variety of laminate types or to a randomly ordered load spectrum.

In contrast to stiffness-based models, strength-based models have an inherent "natural" failure criterion: failure occurs when the applied stress equals or exceeds the residual strength. Strength-based models are often referred to as "wearout" models and generally incorporate the "strength-life equal rank assumption" (SLERA). SLERA assumes that a laminate's fatigue life is proportional to its initial static strength (Hahn and Kim, 1975). From their early use (Halpin, et al., 1972), wearout models have generally been statistical. Two-parameter Weibull functions (Weibull and

Weibull, 1977) have commonly been used to describe the residual strength and probability of failure after an arbitrary number of cycles, as well as life distributions after an indefinitely repeating load sequence. The most successful wearout model, in terms of its predictive capability, is perhaps that developed by Yang et al. (Yang and Liu, 1977; Yang, 1978; Yang and Jones, 1980, 1981,1983; Yang and Du, 1983). In their apparently final work (Yang and Du, 1983), this model showed reasonable correlation with a limited amount of spectrum fatigue test results. However, development of this model has not been continued. This may partly be due to the excessive amount of experimental input that is necessary for the model's characterization.

Based on the above, a strength-based wearout model appears to offer the best near-term promise for developing a reliable predictive methodology for fatigue loaded composite laminates. The challenge is to develop a model that only requires a limited amount of experimental data as input, yet is applicable to randomly ordered load spectra containing a wide variety of load levels.

3. THEORY

3.1 Constant Amplitude Loading

3.1.1 Residual Strength

Consider a single laminate subjected to constant amplitude loading. The residual strength, R(n), initially equals the static strength, R_o, and is assumed to decrease monotonically. If environmental and frequency-based effects are ignored, the rate of strength degradation should depend on R_o, the peak stress magnitude of the loading, S_p, and the stress ratio, R_s. The conventional definition of stress ratio is adopted, i.e., $R_s = S_{min}/S_{max}$, where S_{min} and S_{max} are the minimum and maximum stresses, respectively, in the cycle. Thus, if $-1 < R_s \leq 1$, S_p refers to the magnitude of the tension peak and R_o is the tension strength; otherwise, S_p refers to the magnitude of the compression peak and R_o is the compression strength. Regardless of the stress ratio and peak stress, both S_p and R_o are always positive. Using the above definitions, the general form of the assumed residual strength relation may be written as

$$R(n) = R_o - f(R_o, S_p, R_s)\ n^v \qquad (1)$$

Here, $f(R_o, S_p, R_s)$ describes the rate of strength loss associated with cyclic loading and v is a yet-to-be-determined "strength degradation parameter." The function $f(R_o, S_p, R_s)$ is determined by imposing a failure criterion. It is assumed that the failure will occur when the residual strength, R(n), equals the peak stress magnitude, S_p. By definition, when failure occurs, the number of loading cycles, n, equals the constant amplitude fatigue life, N. Substituting these conditions into Equation (1) gives

$$f(R_o, S_p, R_s) = \frac{R_o - S_p}{N^v} \tag{2}$$

or substituting Equation (2) into Equation (1) .

$$R(n) = R_o - (R_o - S_p)\left(\frac{n}{N}\right)^v \tag{3}$$

Figure 1 illustrates possible residual strength curves as a function of fatigue loading cycles as described by Equation (3). Note that each strength curve begins at the static strength, R_o, and passes through the location defined by the failure criterion, i.e., n=N and $R(n)=S_p$. The path of each curve between these locations is dependent on the value of the strength degradation parameter, v. Linear strength degradation corresponds to v=1; "sudden death" behavior (Chou and Croman, 1978, 1979) is obtained for v>1, and a sudden initial loss in strength is obtained for v<1. The determination of v is based on a comparison of theoretical and experimental fatigue life results and is addressed in a subsequent section.

3.1.2 Probability of Failure

Consider the above equations applied to a set of geometrically "identical" laminates that are subjected to identical loadings. Because strength and life are statistically variable quantities, one would not expect a deterministic equation, such as Equation (3), to be generally accurate. Moreover, a knowledge of the statistical distributions of residual strength and life would be more useful in practical applications. We assume that both the residual strength distribution after an arbitrary number of cycles, and the life distribution after continuous cycling, may be represented by two parameter Weibull functions (Weibull and Weibull, 1977). The two parameters that describe the individual

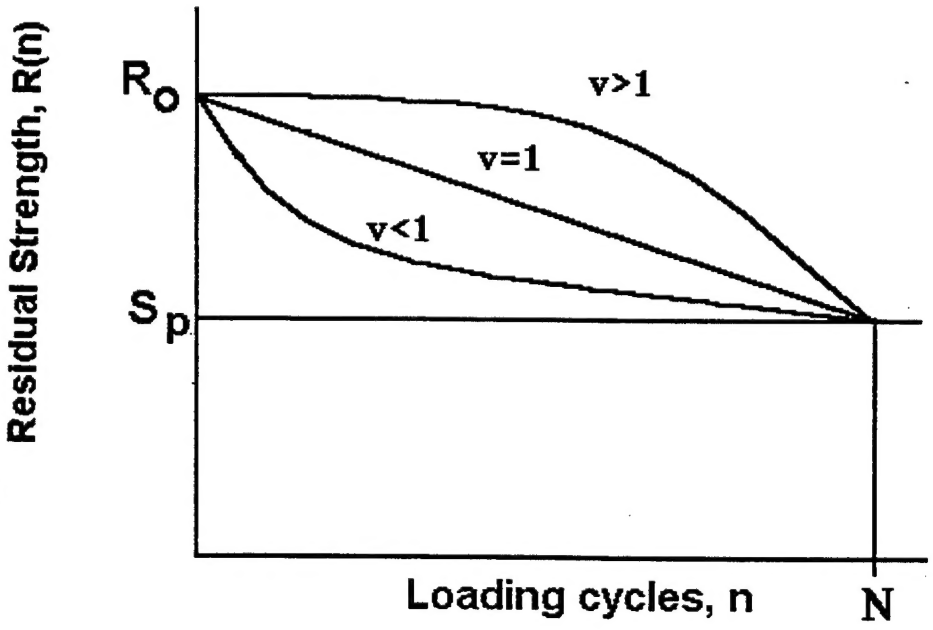

Figure 1. Possible relationships between residual strength and number of loading cycles.

Weibull functions are the scale, which represents the 63.2 percentile of the distribution, and the shape, which describes the degree of scatter in the data. Further, we define R(n), R_o and N to be the 63.2 percentile of their respective distribution functions, i.e., they are all Weibull scale parameters. Figure 1 therefore "tracks" the 63.2 percentile of the strength distribution. To avoid subsequent confusion, we will continue to use the symbols R(n), R_o and N to describe scale parameters described by Eq. (3), and the symbols $\hat{R}(n)$, $\hat{R}_o$ and $\hat{N}$ to describe the residual strength, static strength and life distributions, respectively. Using these definitions, the *static* strength Weibull cumulative distribution function, describing the probability that the initial strength of a laminate is less than or equal to the peak stress magnitude, S_p, is given by

$$P\left[\hat{R}_o \le S_p\right] = 1 - \exp\left[-\left(S_p / R_o\right)^{B_s}\right] \tag{4}$$

where B_s is the shape parameter for static strength (Weibull and Weibull, 1977). Both the shape and scale parameters are obtained from experimental results using the maximum likelihood method (Weibull, 1967). It is recommended that results from a minimum of 5 static strength experiments are used. A similar relation for the Weibull fatigue life distribution is given by

$$P\left[\hat{N} \le n\right] = 1 - \exp\left[-\left(n / N\right)^{B_l}\right] \tag{5}$$

where B_l is the shape parameter for fatigue life. As in the above, it is recommended that a minimum of 5 fatigue life tests are conducted to obtain N and B_l for a given constant amplitude loading.

The probability of failure during constant amplitude fatigue loading, i.e., the probability that the residual strength, $\hat{R}(n)$, is less than the peak stress magnitude, S_p, may also be expressed in the form of a Weibull distribution as

$$P\left[\hat{R}(n) \le S_p\right] = 1 - \exp\left[-\left(S_p / R(n)\right)^{B_f(n)}\right] \tag{6}$$

where $B_f(n)$ is a yet-to-be-determined Weibull shape parameter for residual strength. Substituting the residual strength relation, Equation (3), into Equation (6), the final form of the probability of failure relation for constant amplitude

loading is

$$P[\hat{R}(n) \le S_p] = 1 - \exp\left[- \left(\frac{S_p}{R_o - (R_o - S_p)\left(\frac{n}{N}\right)^v} \right)^{B_f(n)} \right] \tag{7}$$

Figure 2 illustrates, at selected intervals, the strength distributions that are predicted by Eq. (7) for a set of laminates subjected to constant amplitude fatigue loading. A linear strength degradation is assumed (i.e., v=1). The stronger laminates reside in the upper portions of each distribution and the weaker laminates reside in the lower. During fatigue loading, all of the laminates experience a loss in strength. Eventually, the strength of the weaker laminates falls below the peak stress and these laminates are predicted to fail. The failed portion of the distribution is denoted by the darkly shaded areas. As cycling continues, more of the distribution falls below the peak stress and the probability of failure increases.

Next, consider the *shapes* of the distributions in Figure 2. At zero cycles, Eq. (7) must reduce to (4). Thus, the shape parameter for strength at zero cycles, $B_f(0)$, must equal the static shape parameter, B_s. Previous experimental results for residual strength distributions as a function of cycling have shown that these distributions become more disperse during fatigue loading (Yang and Liu, 1977; Yang, 1978; Yang and Jones, 1983). This implies that $B_f(n)$ decreases with increasing cycling. This effect is illustrated schematically in Figure 2; the *range* of values covered by the residual strength distribution expands as the number of loading cycles increases. To account for this effect in the model, it is assumed that $B_f(n)$ initially equals the static shape parameter, and that it degrades linearly to a limiting value of B_l. That is, the relation used to calculate $B_f(n)$ in Equations (6) and (7) is given by

$$\begin{aligned} B_f(n) &= B_s - (B_s - B_l)\ \frac{n}{N} \qquad && n < N \\ B_f(n) &= B_l && n \ge N \end{aligned} \tag{8}$$

We point out that we cannot rigorously justify this assumption on either mathematical or physical grounds. However, for all laminates which we have been able to obtain the appropriate data, we have observed that $B_l < B_s$.

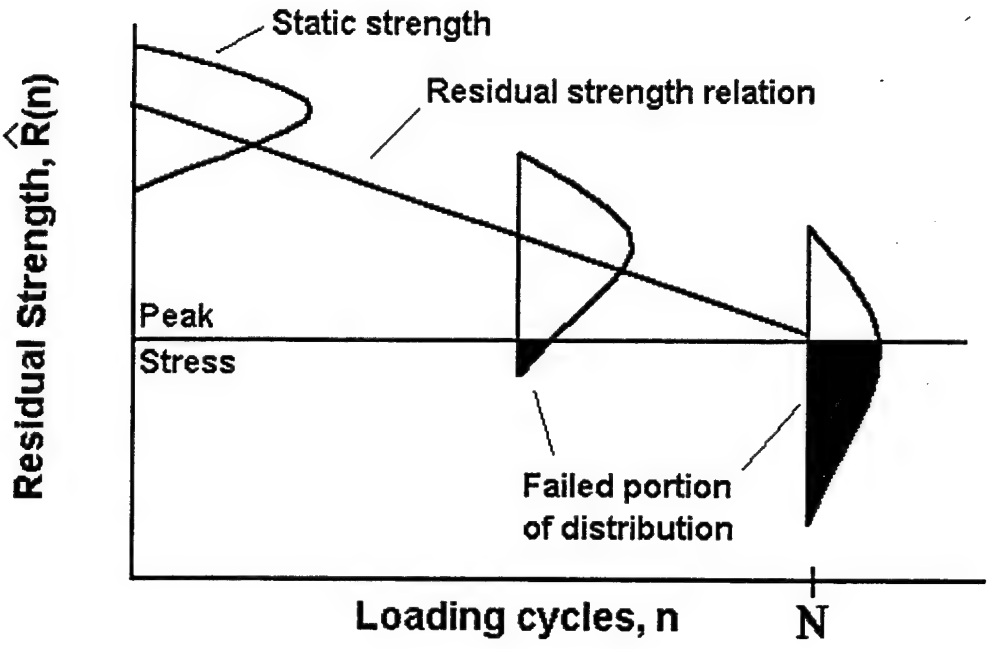

Figure 2. Strength distributions associated with specific residual strength relation.

Also, for the limited amount of data available where residual strength distributions were obtained experimentally after a finite number of loading cycles and where life distributions were also obtained, we have observed that B_1 is less than any of the intermediate residual strength shape parameters. The assumptions of Eq. (8) therefore represent an effort to reproduce observed behaviors *without increasing the number of tests that are required for model characterization*. Utilization of Eq. (8) significantly improves the model's predictive capability as compared to the case where $B_f(n)$ is assumed to always equal B_s; this latter assumption has been used in a number of previous wearout models (Chou and Croman, 1978; Halpin et al, 1972; Yang et al. including Yang and Jones, 1980, 1981, 1983).

3.1.3 Strength Degradation Parameter

The method used to determine the strength degradation parameter, v, consists of comparing the theoretical probability of failure, Equation (7), to the experimentally obtained Weibull distribution for fatigue life, Equation (5), until an "optimum" value is obtained. This is illustrated in Figure 3 using data for Scotchply 1002 cross-ply laminates (Broutman and Sahu, 1972); the experimental curve is plotted based on Weibull distribution fatigue life data since raw data was unavailable.

First, the theoretically predicted probability of failure curves, using Equations (7) and (8) and v values of 0.5, 1.0 and 1.5, were compared to the experimental curve as shown in Figure 3. Based on this type of a comparison, the value of v may be refined to within 0.2. We have found that the "best" values of v, i.e., those that ultimately give the best predictive capability, may be obtained by examining the *upper* portion of the probability of failure curve and refining v to within 0.1. This procedure resulted in a final value of v=1.1 for the laminate of Figure 3. We are currently evaluating whether examining the lower portion of the curve may be used in a secondary fashion to improve the model's predictive capability for early failures.

3.2 Two-Stress Amplitude Fatigue Loading

In this section, the model is extended to two-stress level loadings. Both, the residual strength relation and the probability of failure equation are modified such that they may be applied over each constant amplitude segment.

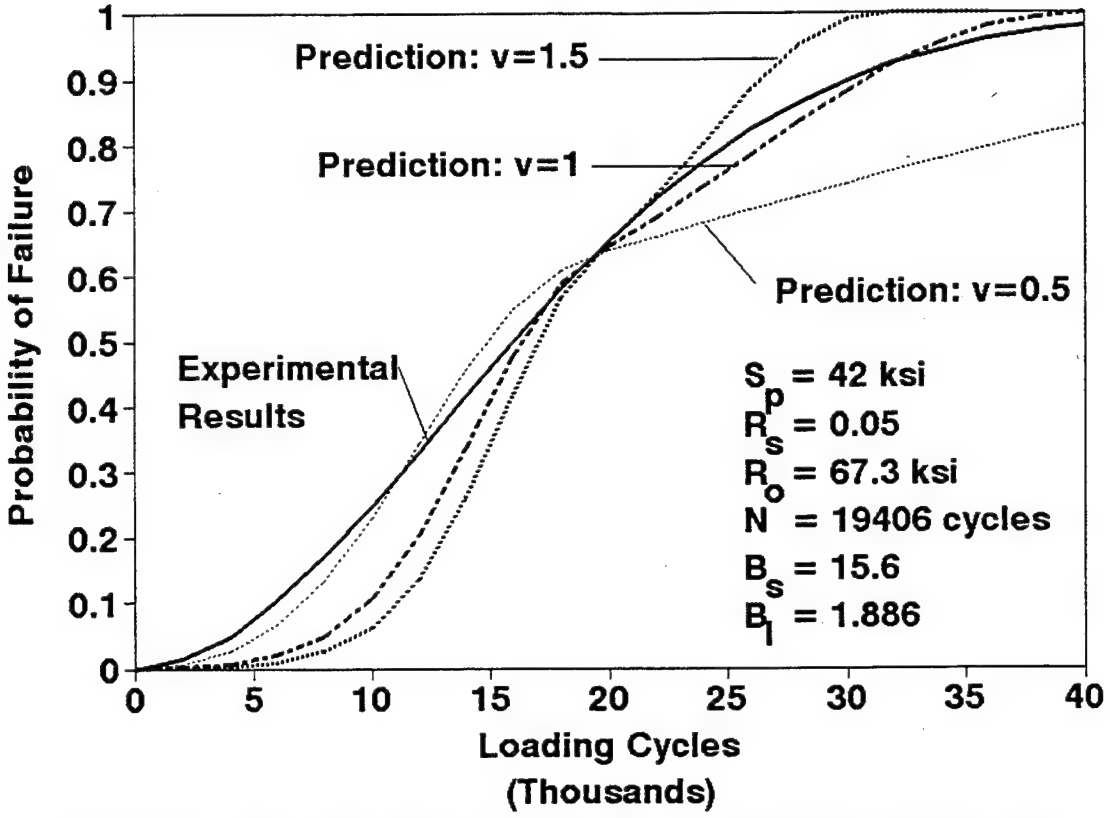

Figure 3. Comparison of observed to predicted results for strength degradation parameters of 0.5, 1.0, and 1.5 for cross-ply glass/epoxy laminates (data from Broutman and Sahu, 1972).

Also, a "cycle mix factor" is added to the model to account for the loss in strength and for life that may result from frequent changes in stress amplitude of the loading. Since N, B_1, and v are dependent on peak stress and stress ratio, it is assumed that they have individually been determined for those peak stress and stress ratio values that define each loading segment.

3.2.1 Residual Strength

Consider a two-stress amplitude fatigue sequence, i.e., two separate constant amplitude loading segments applied sequentially. Assume that the first stress segment consists of n_1 cycles at a peak stress S_1, and that the second segment consists of n_2 cycles at a peak stress S_2. For this example, assume $S_1>S_2$. For a constant amplitude loading defined by a stress level, S_1, let the strength degradation and fatigue life scale parameters be denoted by v_1 and N_1, respectively. Similarly, for a constant amplitude loading defined by a stress level S_2, let the strength degradation and fatigue life scale parameters be denoted by v_2 and N_2, respectively. The scale parameter for residual strength at the end of the first stress segment, and therefore at the beginning of the second stress segment, is $R_1(n_1)$. This strength is given by

$$R_1(n_1) = R_o - (R_o - S_1)\left(\frac{n_1}{N_1}\right)^{v_1} \tag{9}$$

In determining the residual strength after n_2 cycles of the second loading segment, we desire to use the *constant amplitude* residual strength relation characterized by S_2, N_2, v_2, and n_2, i.e.,

$$R_2(n_2) = R_o - (R_o - S_2)\left(\frac{n_2}{N_2}\right)^{v_2} \tag{10}$$

However, the loss-of-strength for the second segment of a two-stress level loading must be calculated beginning from $R_1(n_1)$, and the *rate* of strength loss must be that for the current state of the laminate. That is, except for the special case of a linear degradation law (v=1), the rate at which the strength degrades depends on the amount of previous cycling. Physically, this corresponds to a damage-dependent rate, and has been observed experimentally (Poursartip and Beaumont, 1986).

The way in which the two-stress loading sequence is handled by the model may be most easily described with the aid of Figure 4. In this figure, curve AB illustrates the strength degradation for laminates subjected to constant amplitude loading at stress level S_1, and curve ACD illustrates the strength degradation for laminates subjected to constant amplitude loading at stress level S_2. Both of these curves assume that the specimens are of virgin material and therefore begin at the static strength. Point B represents the strength after n_1 cycles at stress level S_1. Point C represents a location of equivalent strength as that of point B on the constant amplitude loading curve corresponding to stress level S_2. Our model assumes that a laminate that arrived at point B, along path AB, has the same residual strength and essentially the same state of damage as a laminate that arrived at point C along path AC. Applying this idea to the two-stress level sequence, the beginning of the second segment should correspond to point C, and the strength degradation for the second segment itself should occur along path CD. Notice that the curve ACD has a nonlinear strength degradation rate; thus, simply replacing R_o with $R_1(n_1)$ in Eq. (10) will *not* produce the correct result.

To achieve the requisite shift from point B to point C, an "effective" number of cycles, n_{eff}, is introduced. The value of n_{eff} is defined as the equivalent number of loading cycles necessary to produce the same strength loss within the second segment as that predicted to occur within the first segment. Thus, the effective number of cycles may be determined from Equations (9) and (10) by setting $R_1(n_1) = R_2(n_{eff})$ and solving for n_{eff}, i.e., by determining the number of cycles that defines the location of point C in Figure 4. This gives

$$n_{eff} = \left[\frac{R_o - R_1(n_1)}{R_o - S_2} \right]^{1/v_2} N_2 \qquad (11)$$

Referring to Figure 4, Eq. (10) may now be used to predict the strength at the end of segment 2 by replacing n_2 by $n_2 + n_{eff}$. Thus, the scale parameter for residual strength after n_1 cycles at stress S_1 and n_2 cycles at stress S_2 is given by

$$R_2(n_1 + n_2) = R_o - (R_o - S_2) \left[\frac{(n_{eff} + n_2)}{N_2} \right]^{v_2} \qquad (12)$$

Notice that n_{eff} is also the mechanism through which sequencing effects are incorporated into the model. This

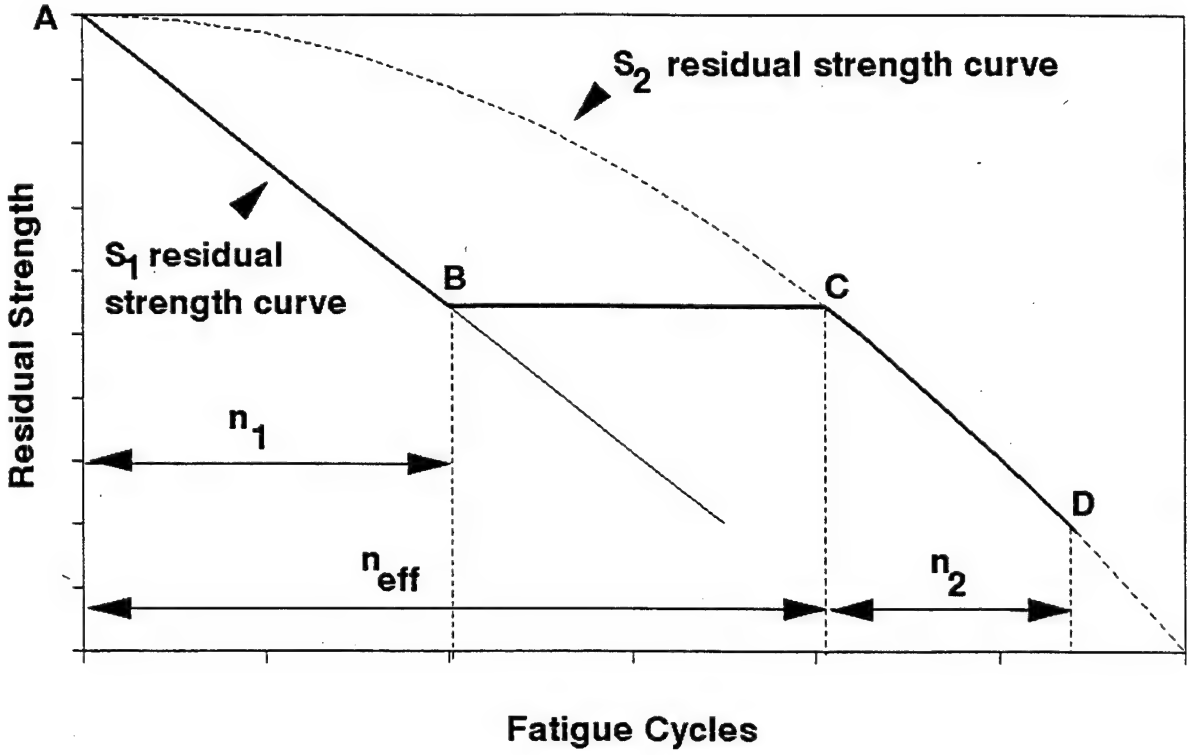

Figure 4. Demonstration of the residual strength relation for two-stress level fatigue.

technique can easily be extended to two-stress level repeating block loadings, as well as multi-stress level loadings.

3.2.2 Probability of Failure

For the two-stress level sequence described above, the probability of failure during the first segment is given by

$$P[\hat{R}_1(n) \le S_1] = 1 - \exp\left[-\left(S_1 / R_1(n)\right)^{B_{f_1}(n)}\right] \tag{13}$$

where $R_1(n)$ is given by Equation (9), with n replacing n_1 and $n \le n_1$. The probability of failure during the second segment is given by

$$P[\hat{R}_2(n_1+n) \le S_2] = 1 - \exp\left[-\left(S_2 / R_2(n_1+n)\right)^{B_{f_2}(n)}\right] \tag{14}$$

where $R_2(n_1+n)$ is given by Eq. (12), with n replacing n_2, and n is interpreted as the current number of cycles in the second segment.

To determine the probability of failure after an arbitrary number of cycles, a "tracking" technique is adopted by the model. That is, suppose in the current example that $S_2 << S_1$ and $N_2 >> N_1$. Under these circumstances, it is possible that the probability of failure at the beginning of segment 2, as predicted by Eq. (14), will be *less* than at the end of segment 1 as predicted by Equation (13). When this occurs, the model stores the probability of failure at the end of segment 1. The probability of failure during segment 2 is taken to be the greater of that predicted at the end of segment 1 or that predicted by Eq. (14). This technique is also readily extended to two-stress level repeating block or multi-stress level loadings.

The equations defining the residual strength shape parameter are also readily extended to two-stress and multi-stress level loadings. For the first loading segment, Eq (8) may be rewritten as

$$B_{f_1}(n) = B_s - (B_s - B_{1_1}) \frac{n}{N_1} \qquad if\ B_{f_1} > B_{1_1}\ and\ n < N_1 \tag{15a}$$

otherwise,

$$B_{f_1} = B_{l_1} \tag{15b}$$

where the subscript "1" designates values corresponding to the first load level. A generalization of Equation (15) for multi-stress level loadings yields

$$\begin{aligned} &If\ B_{l_j} < B_{f_{j-1}}(n_{j-1}) \\ &Then\ B_{f_j}(n) = B_s - \sum_{i=1}^{j-1} (B_s - B_{l_i})\ \frac{n_i}{N_i} - (B_s - B_{l_j})\ (\frac{n}{N_j}) \end{aligned} \tag{16a}$$

$$\begin{aligned} &If\ B_{l_j} < B_{f_{j-1}}(n_{j-1})\ and\ B_{f_j}(n)\ [as\ given\ by\ (16a)] \le B_{l_j} \\ &Then\ B_{f_j}(n) = B_{l_j} \end{aligned} \tag{16b}$$

$$\begin{aligned} &If\ B_{l_j} \ge B_{f_{j-1}}(n_{j-1}) \\ &Then\ B_{f_j}(n) = B_{f_{j-1}}(n_{j-1}) \end{aligned} \tag{16c}$$

In the above, "j" is the current load segment, n is the current number of cycles within that segment, $B_{f_j}(n)$ is the current residual strength shape parameter, $B_{f_k}(n_k)$ is the residual strength shape parameter at the end of load segment "k", and B_{l_k} is the fatigue life shape parameter corresponding to load segment "k."

If the fatigue life shape parameter of the current segment, B_l, is less than the current value of $B_f(n)$, then these equations linearly degrade $B_f(n)$ to a limiting value of B_l. However, if the fatigue life shape parameter of the current segment is *greater* than the current value of $B_f(n)$, then these equations enforce the physical condition that $B_f(n)$ cannot increase. Rather, the value of $B_f(n)$ is kept at its current value for the load segment.

3.2.3 Cycle mix

The residual strength and fatigue life of composite laminates have been observed to decrease more rapidly when the loading sequence is repeatedly changed after only a few loading cycles (Farrow, 1989). This was classified by Farrow (1989) as a "cycle mix effect." For illustration, consider Figure 5, where large block and small block loading sequences are compared. In this figure, the large block loading consists of 10,000 cycles at the low stress level followed by 100 cycles at the higher stress level, while the small block loading contains 1,000 cycles at the low stress followed by 10 cycles at the high stress. Note that after 10,100 cycles, both the large block and small block

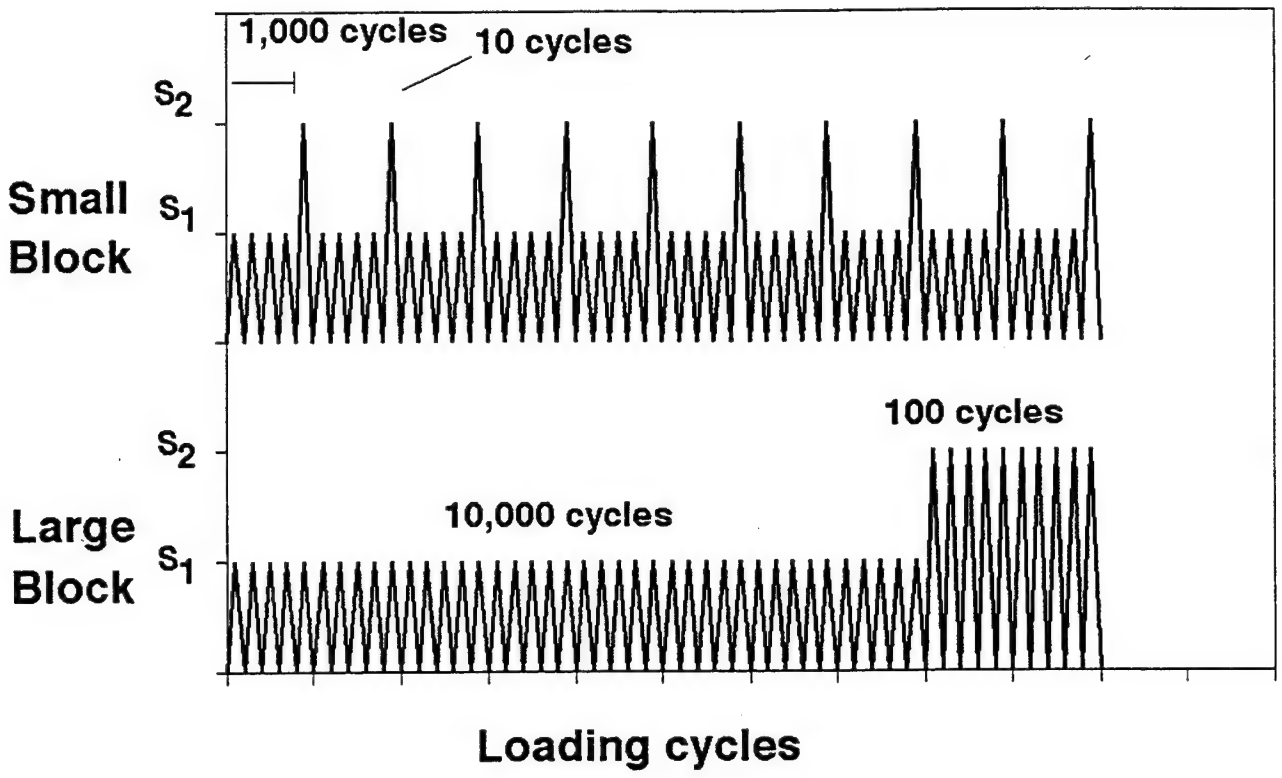

Figure 5. Illustration of loading sequences with small cycle blocks, top, and large cycle blocks, bottom.

loadings contain the same number of cycles at each stress level. However, it has been observed (Farrow, 1989) that laminates that experience small block loadings have reduced average fatigue lives as compared to laminates that are subjected to large block loadings.

It is our belief that the cycle mix effect is a result of the damage that occurs during those "transition cycles," between different constant amplitude segments, where the magnitude of the mean stress increases. This effect is accounted for in the model through application of a "cycle mix factor." The cycle mix factor is applied *only when the magnitude of the mean stress increases* from one segment to the next. *During these transition cycles*, the scale parameter for residual strength is degraded according to the relation

$$R(n) \rightarrow R(n) - CM \tag{17}$$

where CM is the cycle mix factor, given by

$$CM = C_m R_o \left[\frac{\Delta S_{mn}}{R(n)} \right]^{\left(\frac{\Delta S_p}{\Delta S_{mn}} \right)^2} \tag{18}$$

In this equation, ΔS_p and ΔS_{mn} are the change in the peak stress magnitude and mean stress, respectively, during the transition between stress levels. The conventional definition of mean stress is utilized, i.e.,

$$S_{mn} = (S_{max} + S_{min}) / 2 \tag{19}$$

The cycle mix constant, C_m, is determined by comparing fatigue life data from small block and large block two-stress level fatigue loadings to predicted results. A single value of C_m is chosen that gives the best agreement based on the 63.2 percentile of each distribution. We have observed that the cycle mix factor may be negligibly small for certain laminates (Schaff and Davidson, 1994a). Our results also suggest that cycle mix is a significant contributor to strength loss only when the ratio of loading cycles, n, to fatigue life, N, is less than 0.001. In instances where n/N is greater than 0.001, the strength loss due to the cycle mix effect is generally small; thus, C_m is small and the cycle mix factor is likely not required. Of course, the cycle mix factor may be included for all loadings; exclusion of this effect for $n/N > 0.001$ is suggested only to reduce the required experimental input to the model.

Finally, we point out that Eq. (18) was obtained through evaluation of a number of possible relationships comprised of nondimensional groupings of suitable governing parameters. Of those expressions evaluated, Eq. (18)

gave the best results, in terms of the model's predictive capability, for a wide variety of laminates and loadings. We are currently performing a more extensive investigation of the effect of cycle mix for a range of materials, layups, and geometries.

4. APPLICABILITY

Although the emphasis of the preceding discussion may have given the impression that the model is applicable only to uniaxial loading, there is no loss in generality in applying the formulation to multiaxially, proportionately loaded laminates. That is, proportional loading can be characterized by a single parameter and this is the only assumption made on the loading in the model's derivation. Similarly, the model can be applied to complex geometries if the appropriate characterization testing is performed. For example, tests could be performed on a scale version of a local configuration where failure is expected, and the loading acting on this local feature could be defined using finite element results from the full scale structure.

5. RESULTS

In this section, the model is evaluated through a comparison of predicted and observed fatigue life distributions for glass/epoxy and graphite/epoxy laminates subjected to various constant amplitude and two-stress level uniaxial fatigue loadings. The constant amplitude fatigue data are primarily used for model characterization; however, the degree to which the model can reproduce these results provides some measure of its accuracy. Two-stress level results are used to evaluate the model's ability to account for both sequencing and cycle mix effects.

5.1 Sequencing Effects

All evaluations of the model's accuracy for predicting sequencing effects were performed using the data of Broutman and Sahu (1972) on cross-ply, glass/epoxy laminates. Constant amplitude, tension-tension fatigue tests were performed at four different peak stresses; various low-high and high-low tests were performed using variations of these four stress levels and various block sizes. In all cases, the second loading block was a "runout block," i.e., of sufficient length that all laminates failed. Much of this same data was also used by Yang and Jones (1981) to

evaluate their model. All of the two-stress level results of Broutman and Sahu (1972) are compared to predictions from our model and, for comparison, predictions by the Palmgren-Miner rule (Palmgren, 1924; Miner, 1945), based on the 50th percentile. Results from Yang and Jones' (1981) model are included where available.

The constant amplitude results of Broutman and Sahu (1972) were utilized to determine values of N, B_1 and v corresponding to each of their test stress levels. This was accomplished using the previously described techniques and the resulting parameters are summarized in Table 1. Figures 6 through 9 compare the model's predicted life distributions to the experimentally obtained Weibull distributions [cf. Eq. (5)]. In general, the correlation is quite good. As would be expected from our method of determining v, the largest discrepancies between the predicted and observed results occur at the lower end of the probability of failure curves. In these figures, all of the experimental distributions are obtained using the maximum likelihood method (Weibull, 1967) and are based on at least 30 data points. In subsequent figures showing two-stress level results, the experimental probability of failure curves are plotted using log-normal cumulative distributions based on the mean lives and standard deviations presented by Broutman and Sahu (1972). Also, in subsequent figures, "predictions" refer to those by the model presented herein and "Yang's model" refers to results taken directly from Yang and Jones (1981).

Data from six high-low, small first block loadings were presented by Broutman and Sahu (1972) and the comparison between theory and experiment is presented in Figures 10-15. We define a "small first block loading" as one in which $n_1/ N_1 < 0.2$, where n_1 is the number of cycles in the first segment and N_1 is the scale parameter for life for the constant amplitude loading that defines this segment. The discontinuity in slope in our model's predictions occurs when $B_f(n)$ reaches its limiting value. The three loading cases of Figures 10-12 were also evaluated by Yang and Jones (1981) and essentially similar predictive capability is observed for the two models. Predictions of mean life by the Palmgren-Miner rule are comparable to those by the wearout models for all of these loading cases.

There is no single cause to which we can attribute the relatively poor correlation of Figures 14 and 15 as compared to that of Figures 10-13. The poor initial correlation of the constant amplitude predictions at 42 ksi and 35 ksi stress levels shown in Figures 8 and 9 are certainly contributory. However, this does not explain the reasonably good

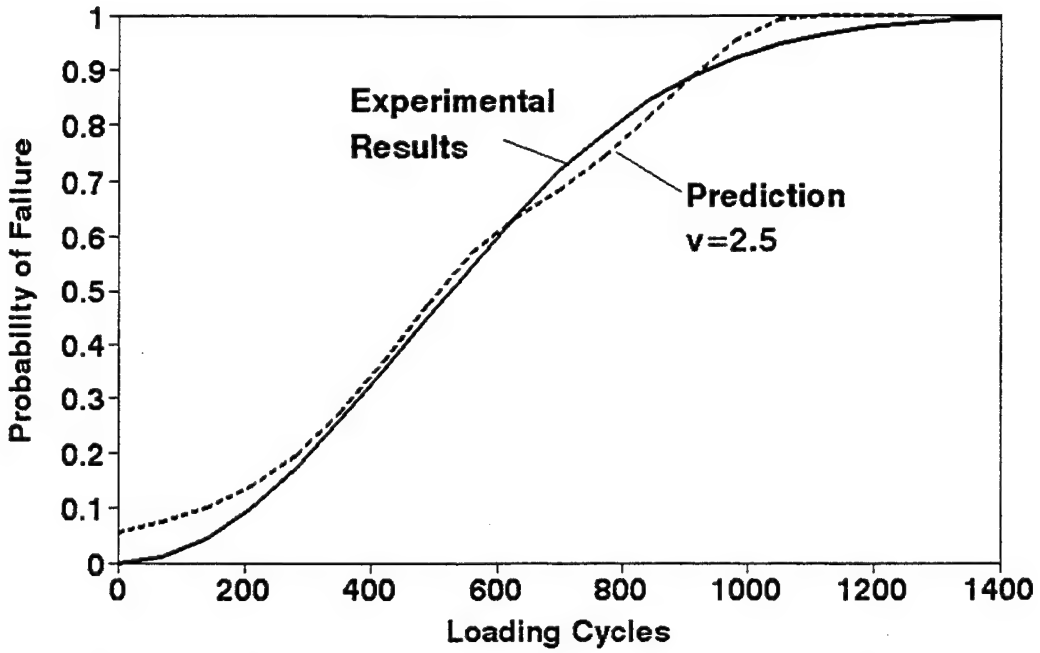

Figure 6. Comparison of predicted and experimental results for glass/epoxy cross-ply laminates subjected to constant amplitude loading with a maximum stress of 56 Ksi (data from Broutman and Sahu, 1972).

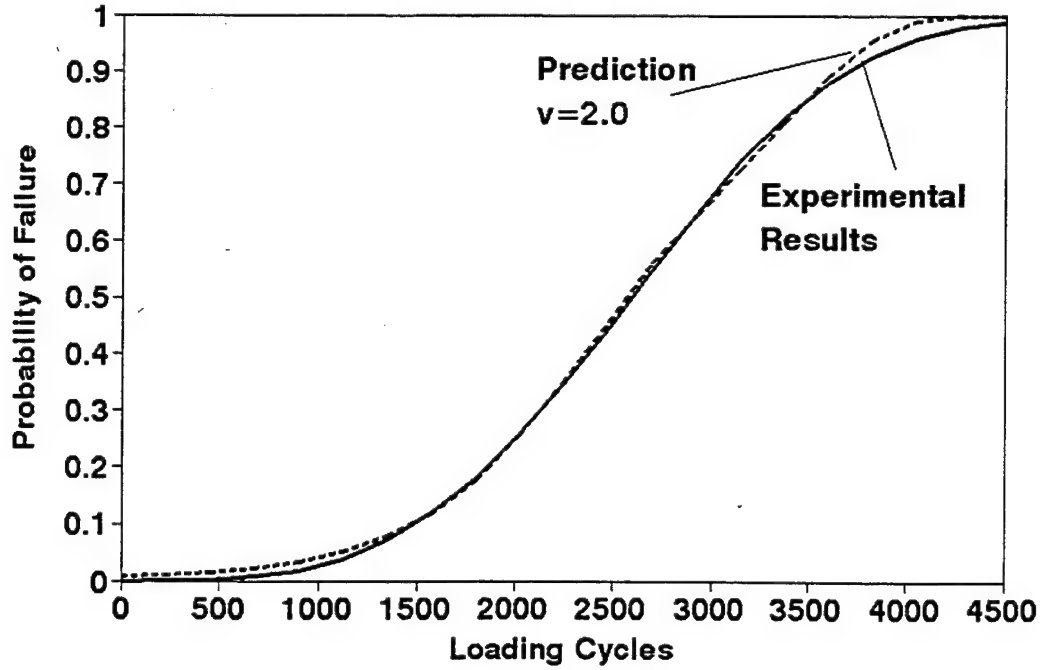

Figure 7. Comparison of predicted and experimental results for glass/epoxy cross-ply laminates subjected to constant amplitude loading with a maximum stress of 49 Ksi (data from Broutman and Sahu, 1972).

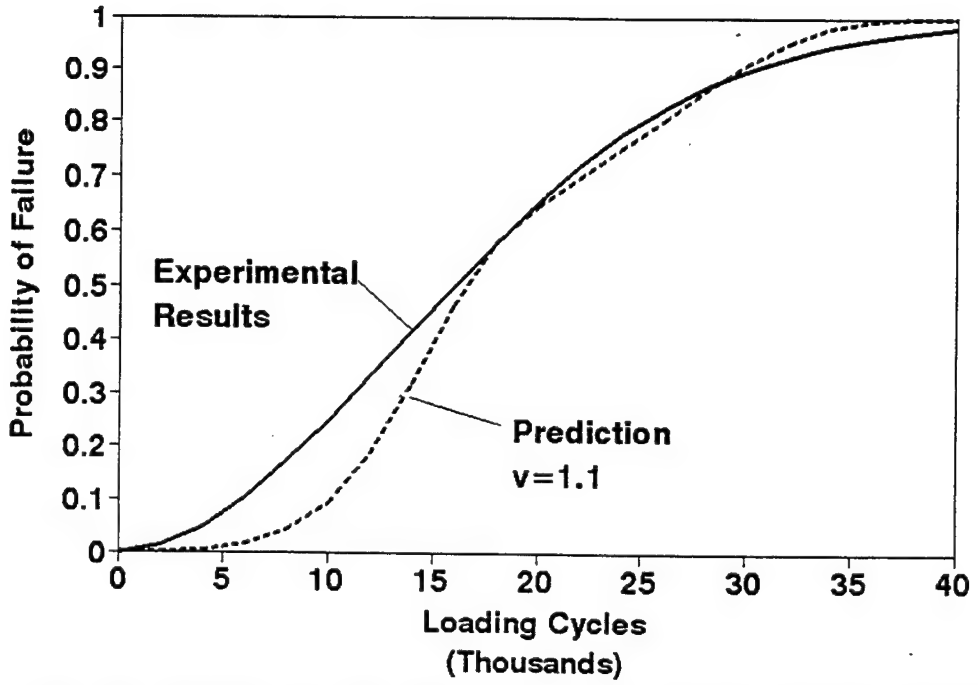

Figure 8. Comparison of predicted and experimental results for glass/epoxy cross-ply laminates subjected to constant amplitude loading with a maximum stress of 42 Ksi (data from Broutman and Sahu, 1972).

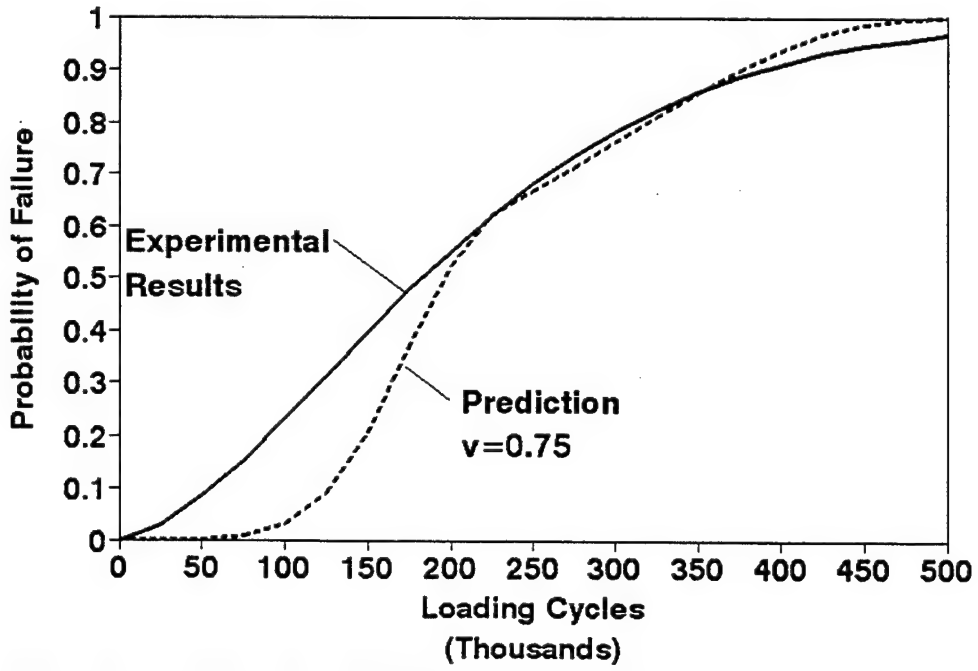

Figure 9. Comparison of predicted and experimental results for glass/epoxy cross-ply laminates subjected to constant amplitude loading with a maximum stress of 35 Ksi (data from Broutman and Sahu, 1972).

correlation for the loading of Figure 12 as opposed to that of Figure 14; considering the constant amplitude fatigue results, one would expect similar correlation between theory and experiment for these two load cases. Part of the discrepancy is perhaps due to the inherent variability of the data. Within the present construct of the model, better (or worse) correlation can be obtained by assuming different functional dependencies of $B_f(n)$. For example, if $B_f(n)$ decreases more rapidly to (or beyond) its limiting value of B_1, then better correlation is obtained in Figures 14 and 15, although this results in worse correlation in Figures 11 and 12. This may imply that the change in the fatigue strength shape parameter with increasing cycling is somewhat more complex than that assumed by Equations (15) and (16). To obtain better predictions for two-stress level runout fatigue, without altering the fundamental nature of the model, would therefore require a more comprehensive experimental assessment of the change in $B_f(n)$ with load cycling and/or an evaluation of various linear and nonlinear degradations in $B_f(n)$ that are perhaps dependent upon the stress level. To date, we have not pursued either of these options. We believe that the significant increase in characterization testing required for the former option would make the model non-viable for practical applications. As will be shown in Part II of this work, the predictive capability of the model in its present form is quite good for realistic, randomly ordered load spectra; this is the primary reason we have not as yet addressed possible alterations in the model associated with the latter option. It will be shown in the next section that the general accuracy of the model for realistic load spectra is partially due to the fact that the sequencing effects evident in two-stress level runout fatigue are somewhat "overshadowed" by the loss in strength and life that is associated with a large number of changes in the stress amplitude of the loading.

Table 1. Model Parameters for Constant Amplitude Fatigue Loading

Maximum Stress (ksi)	Minimum Stress (ksi)	N (cycles)	B_1	v
56	2.80	626	2.089	2.5
49	2.45	2888	3.436	2.0
42	2.10	19406	1.886	1.1
35	1.75	230419	1.595	0.75

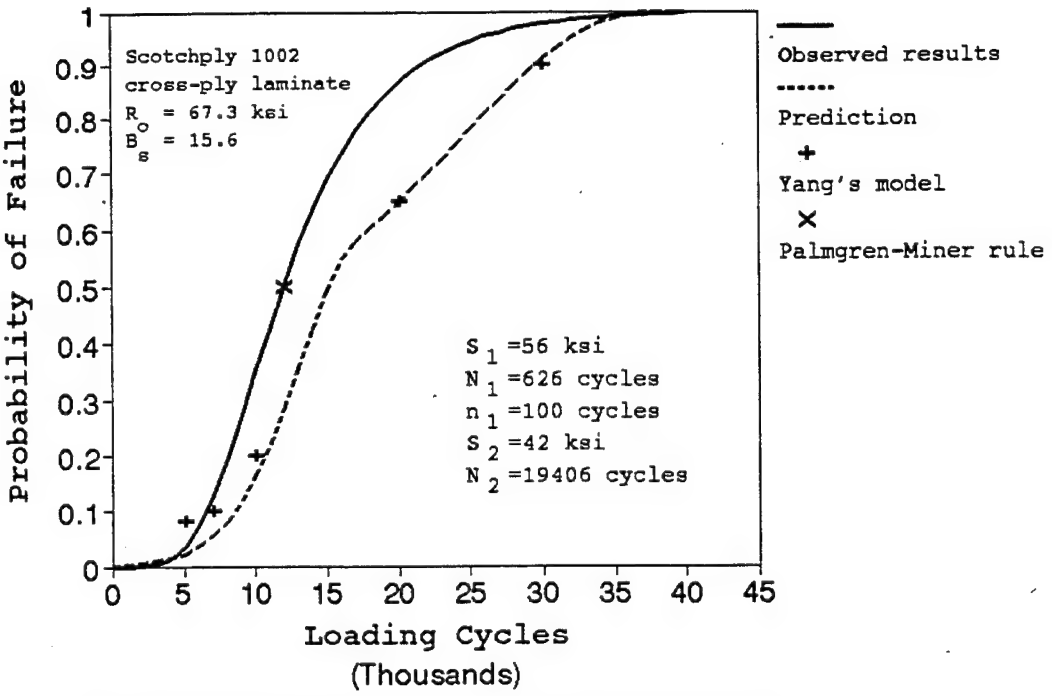

Figure 10. Comparison of predicted and observed results for a high-low small first block loading.

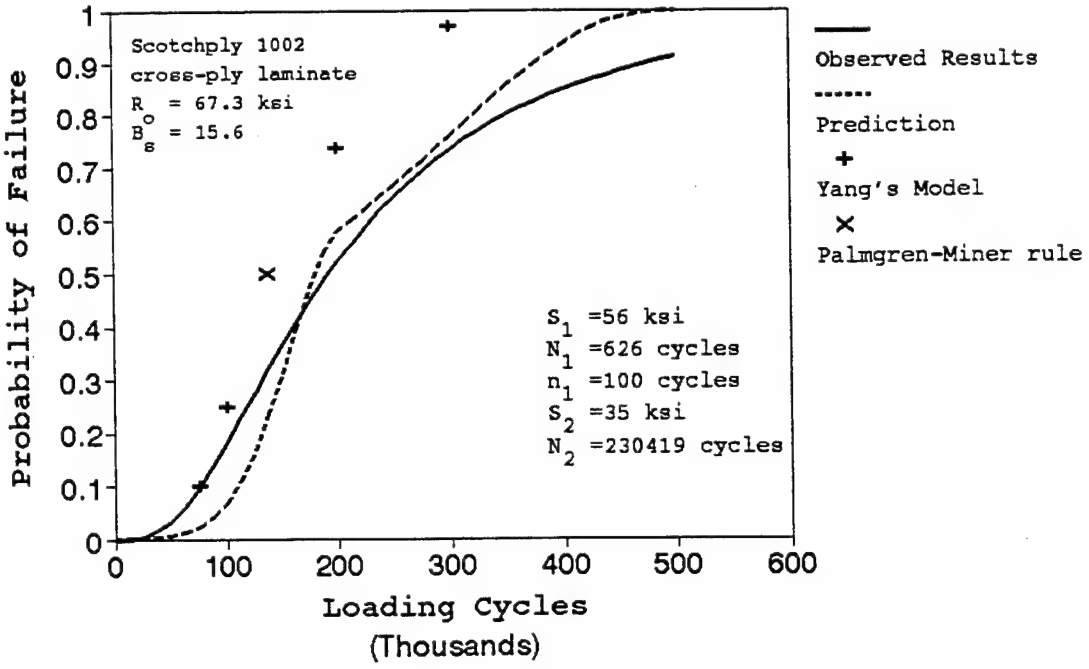

Figure 11. Comparison of predicted and observed results for a high-low small first block loading.

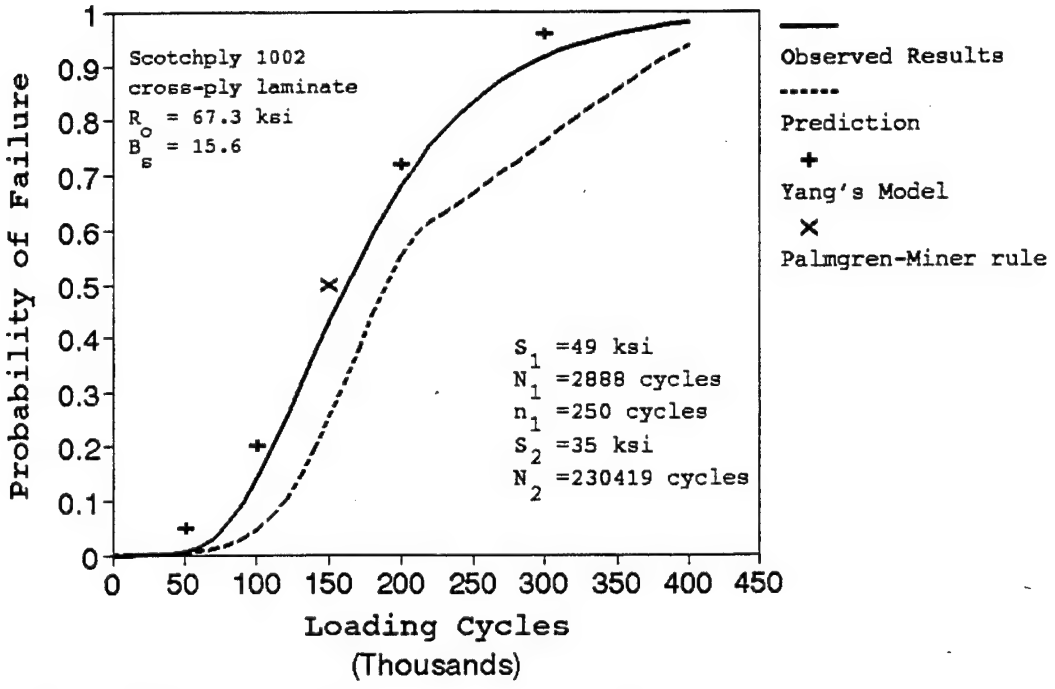

Figure 12. Comparison of predicted and observed results for a high-low small first block loading.

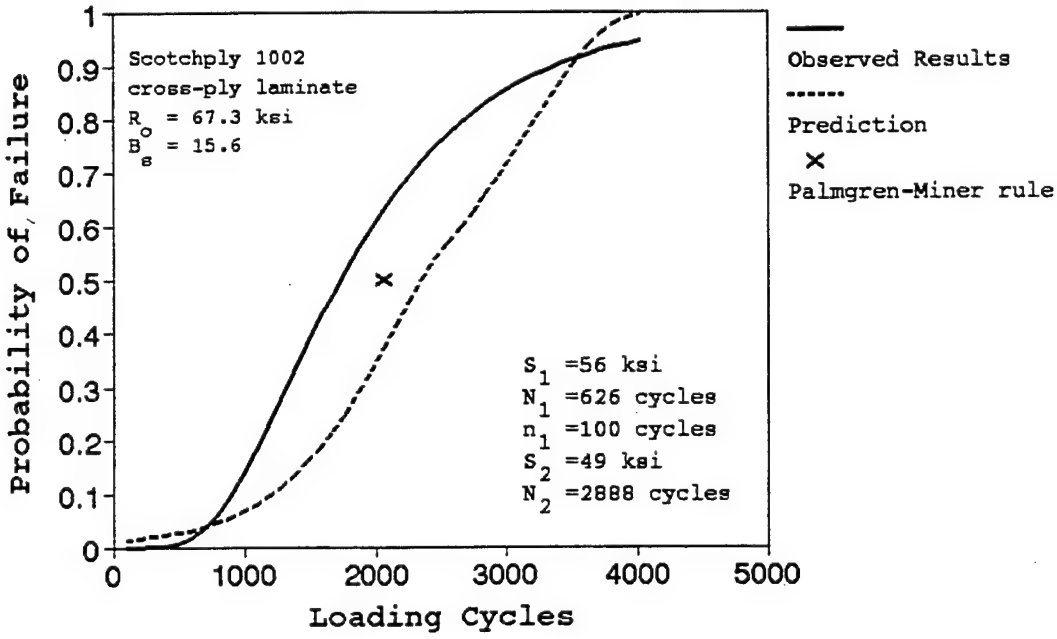

Figure 13. Comparison of predicted and observed results for a high-low small first block loading.

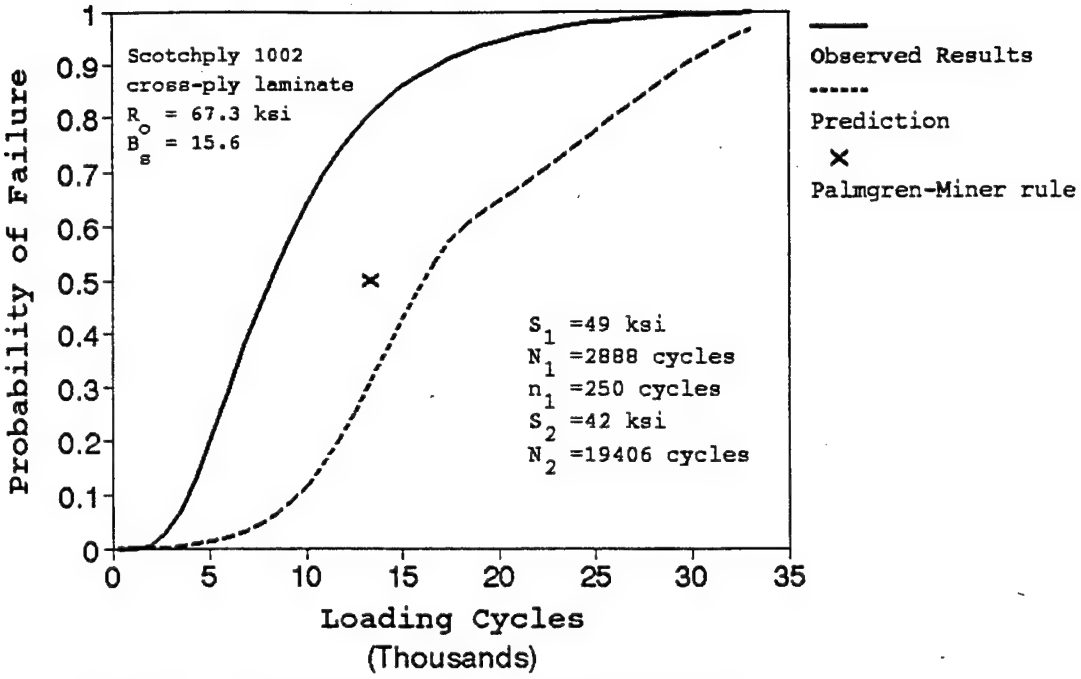

Figure 14. Comparison of predicted and observed results for a high-low small first block loading.

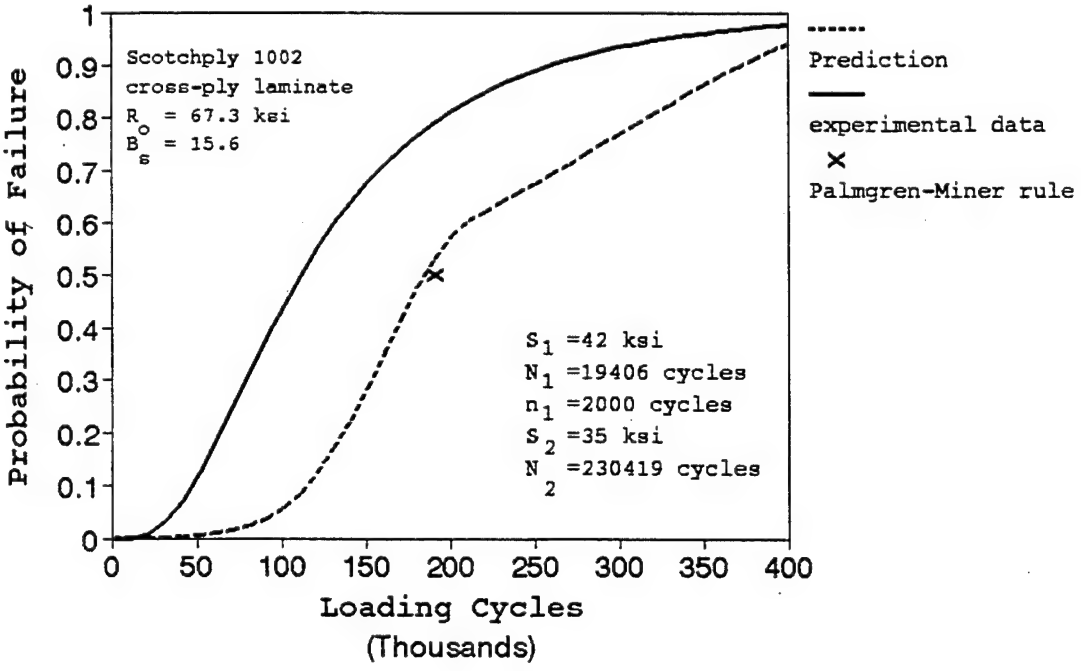

Figure 15. Comparison of predicted and observed results for a high-low small first block loading.

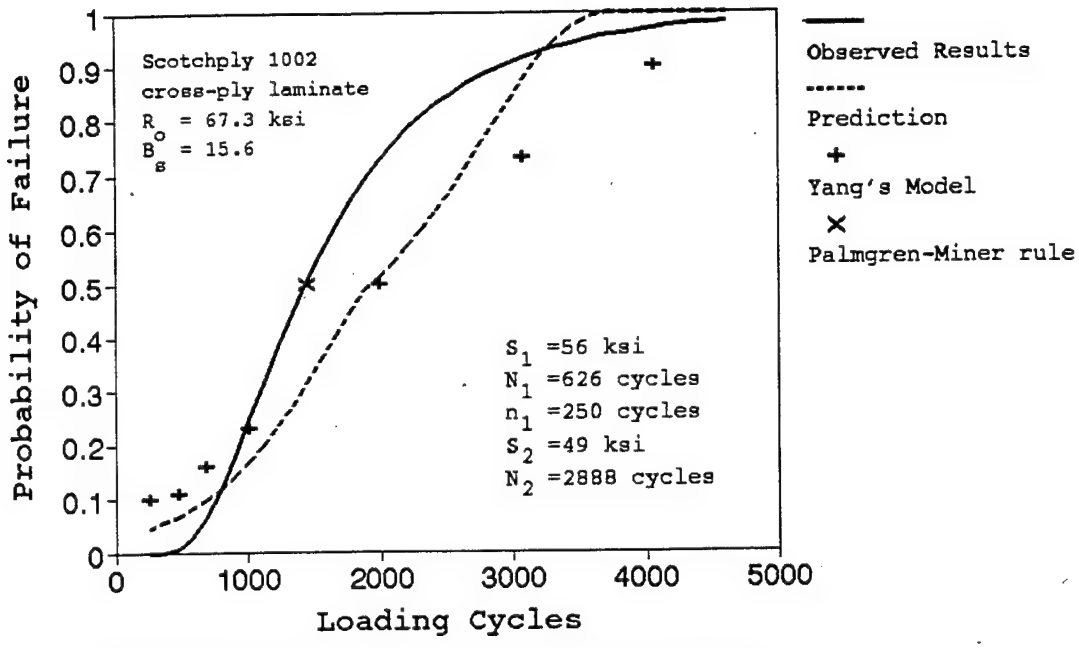

Figure 16. Comparison of predicted and observed results for a high-low large first block loading.

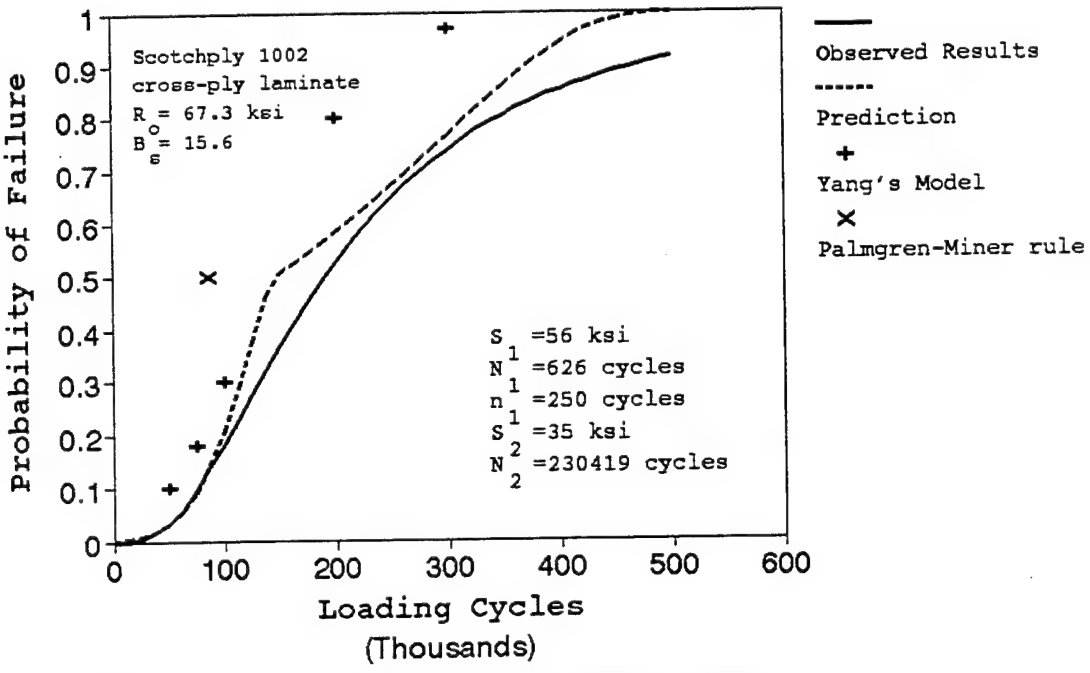

Figure 17. Comparison of predicted and observed results for a high-low large first block loading.

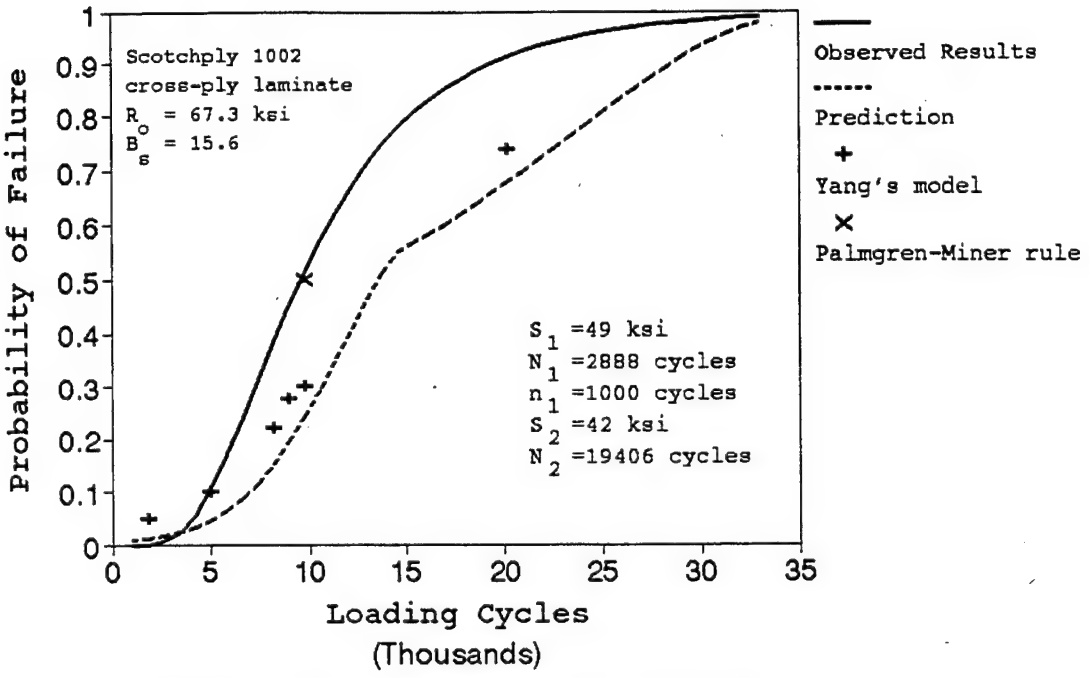

Figure 18. Comparison of predicted and observed results for a high-low large first block loading.

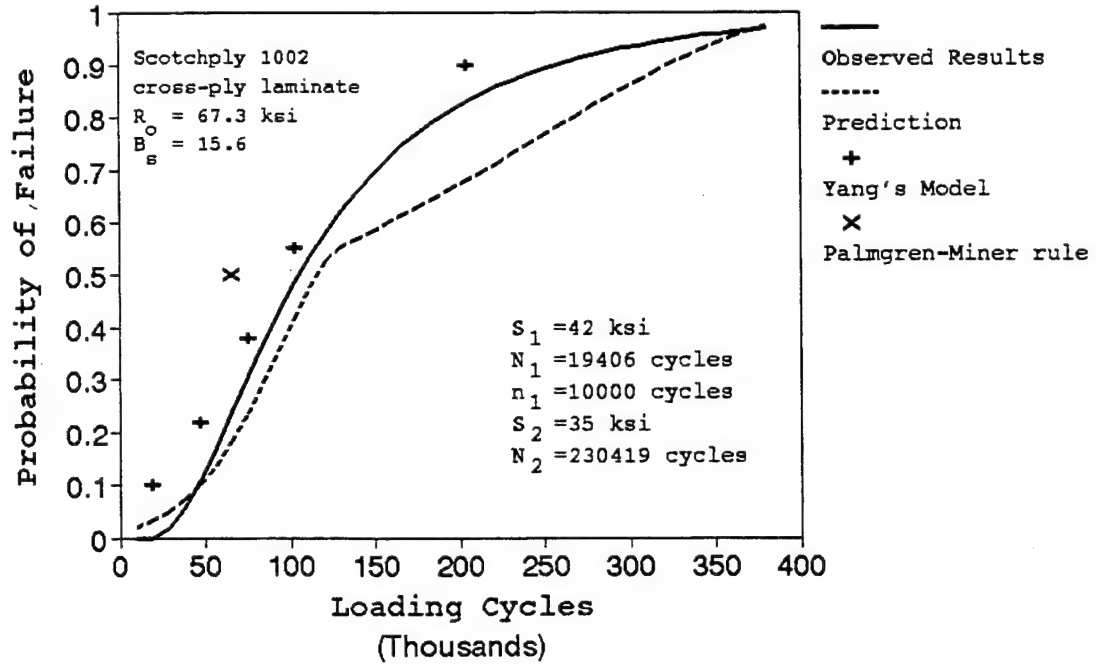

Figure 19. Comparison of predicted and observed results for a high-low large first block loading.

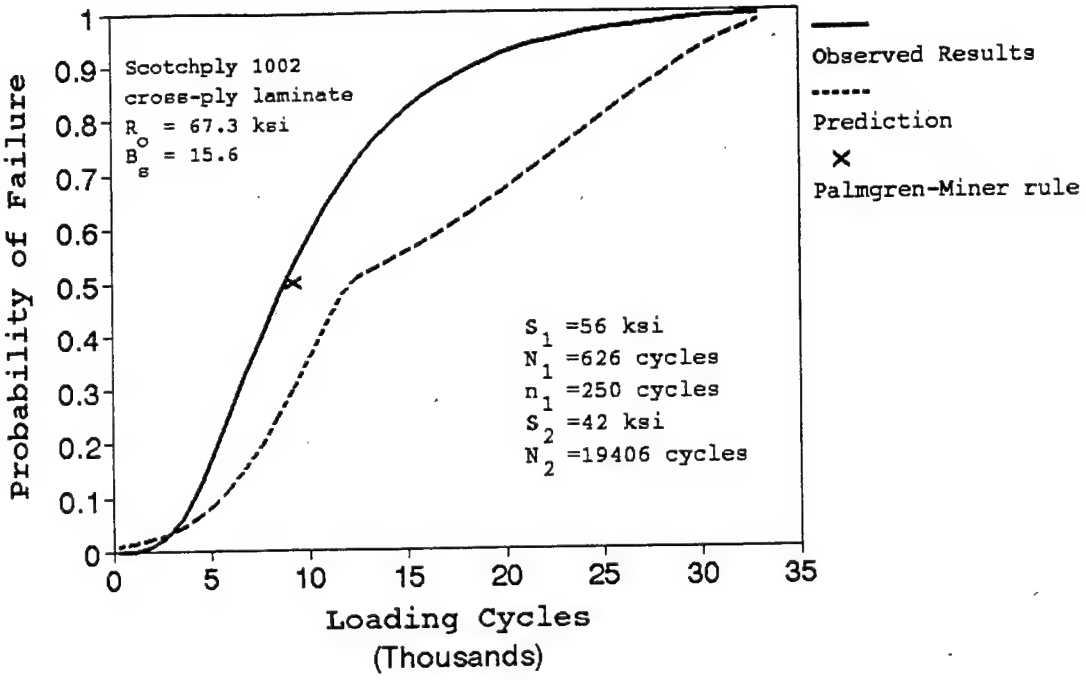

Figure 20. Comparison of predicted and observed results for a high-low large first block loading.

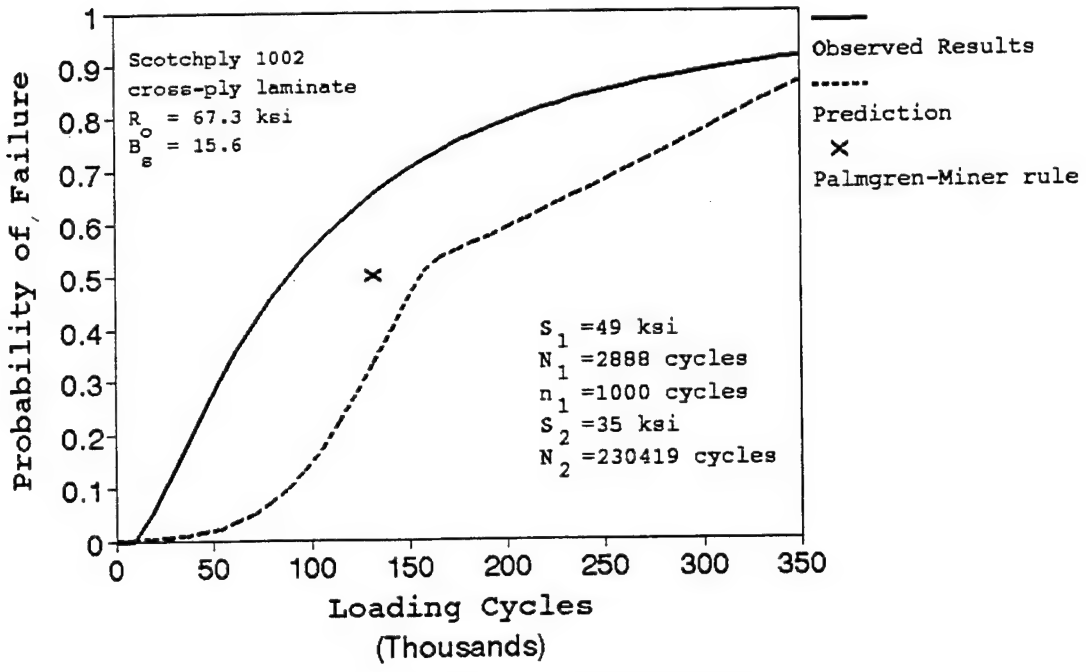

Figure 21. Comparison of predicted and observed results for a high-low large first block loading.

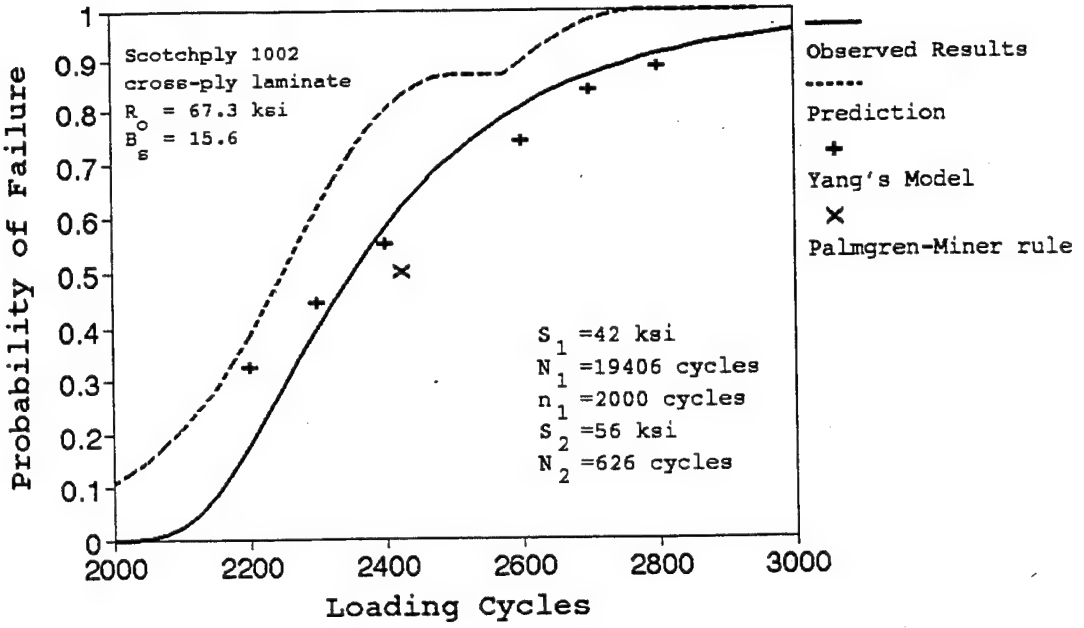

Figure 22. Comparison of predicted and observed results for a low-high small first block loading.

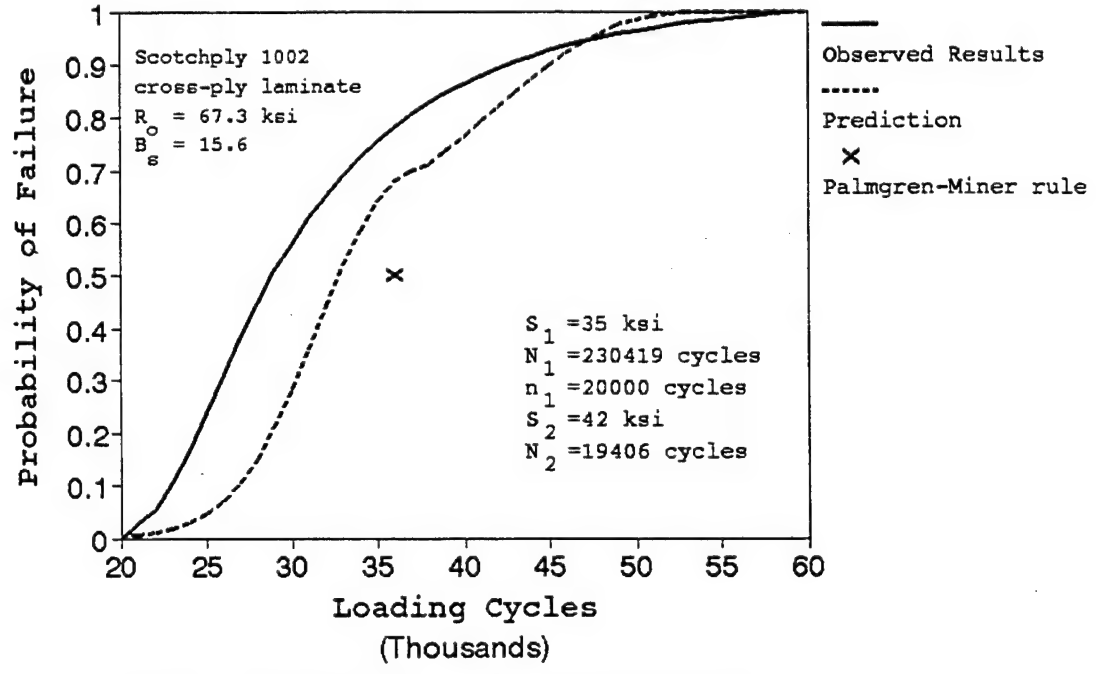

Figure 23. Comparison of predicted and observed results for a low-high small first block loading.

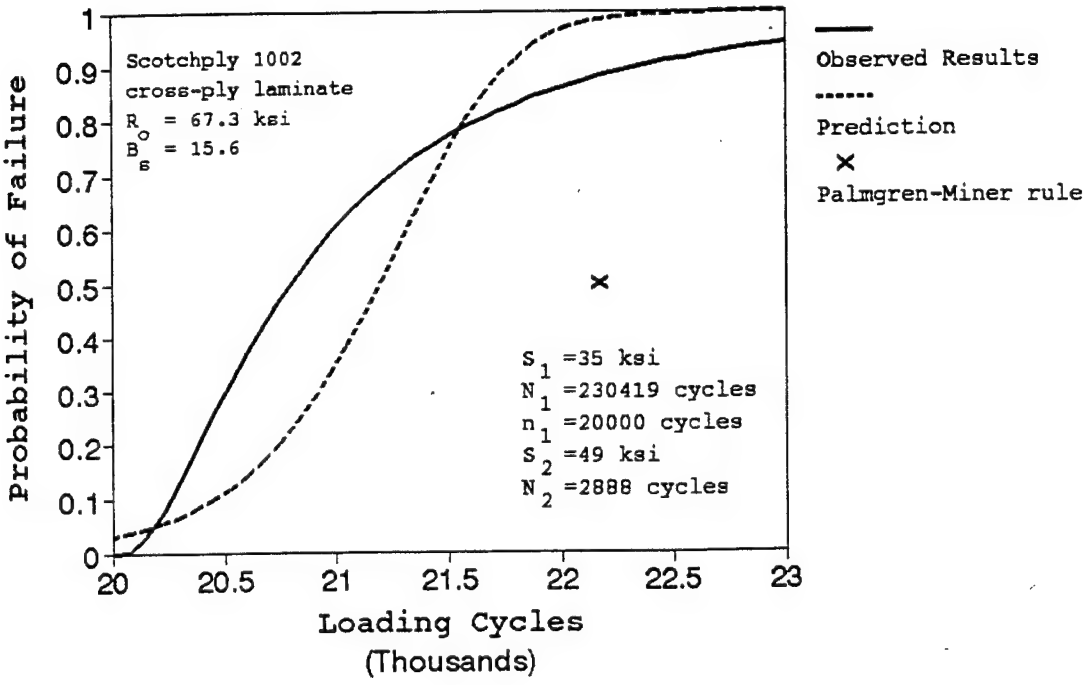

Figure 24. Comparison of predicted and observed results for a low-high small first block loading.

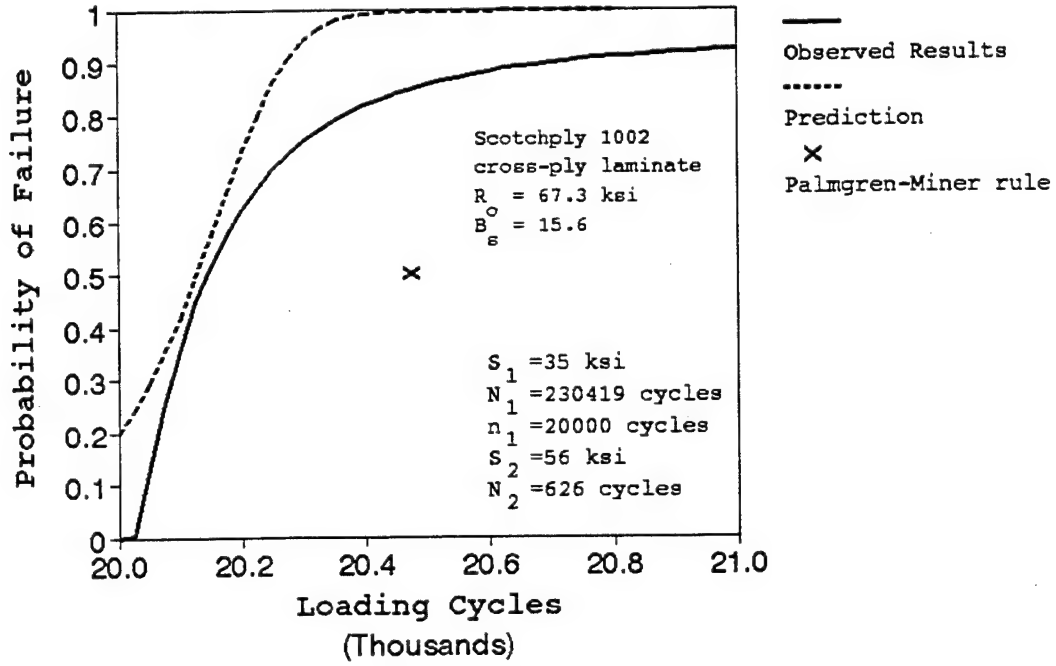

Figure 25. Comparison of predicted and observed results for a low-high small first block loading.

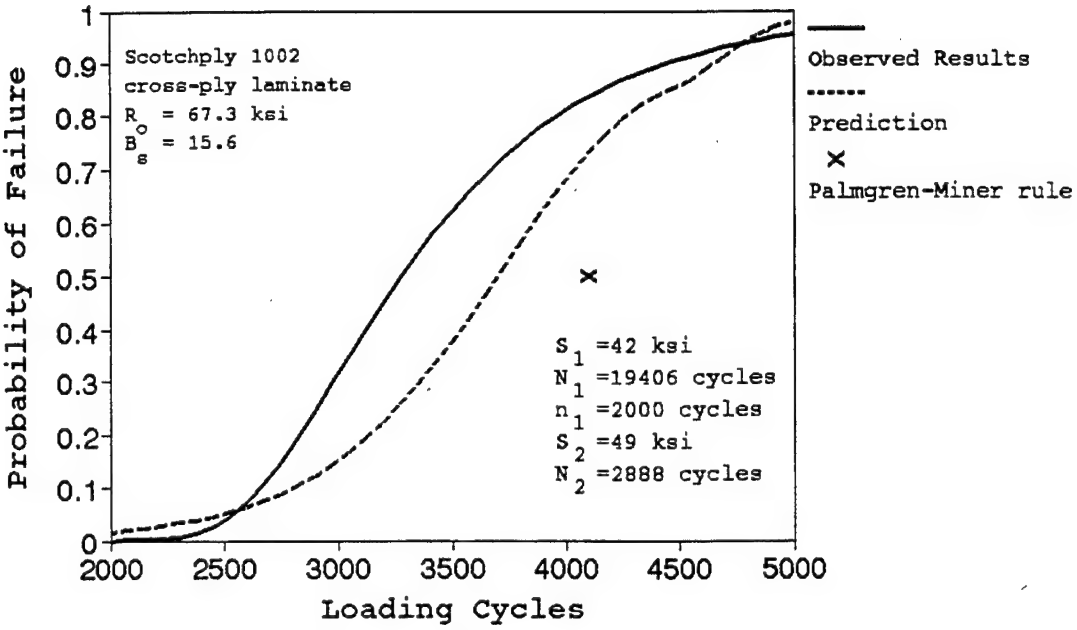

Figure 26. Comparison of predicted and observed results for a low-high small first block loading.

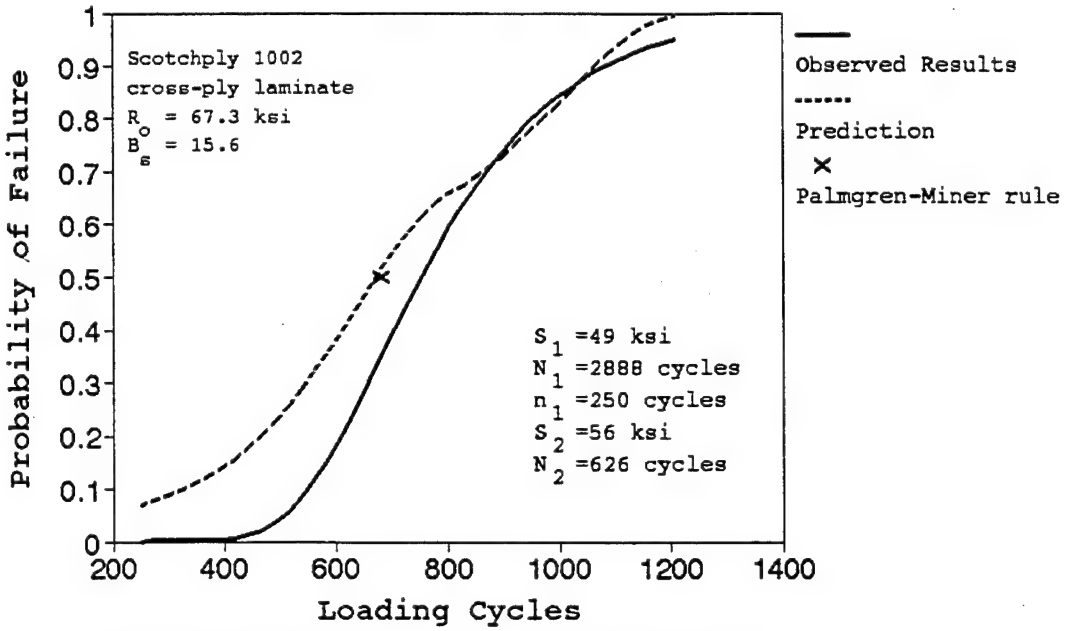

Figure 27. Comparison of predicted and observed results for a low-high small first block loading.

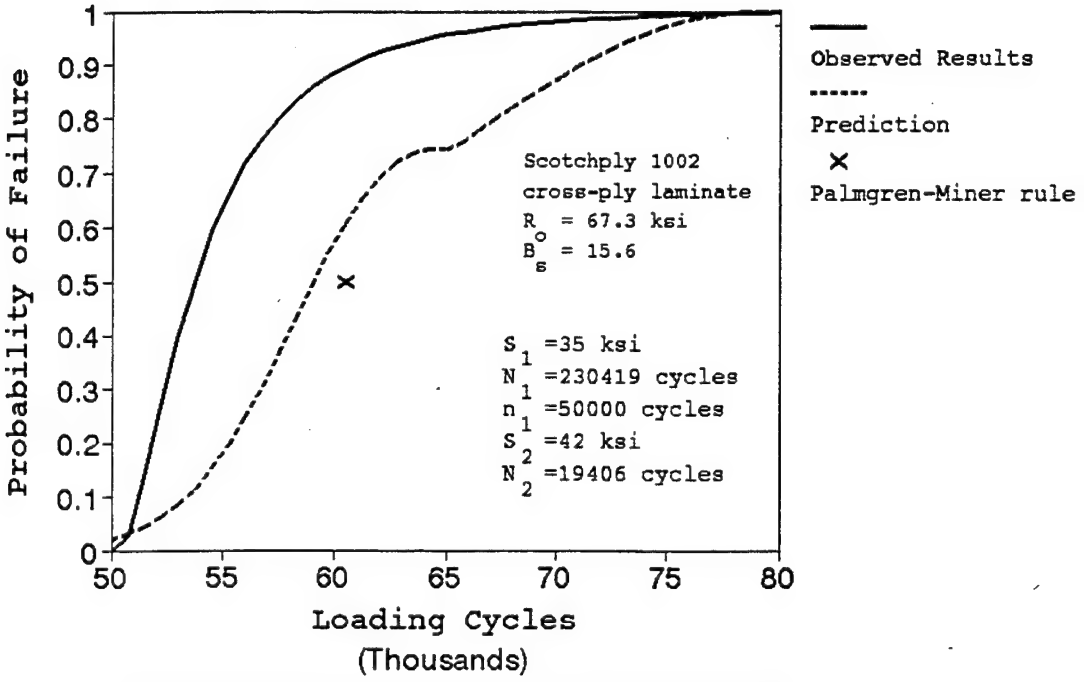

Figure 28. Comparison of predicted and observed results for a low-high large first block loading.

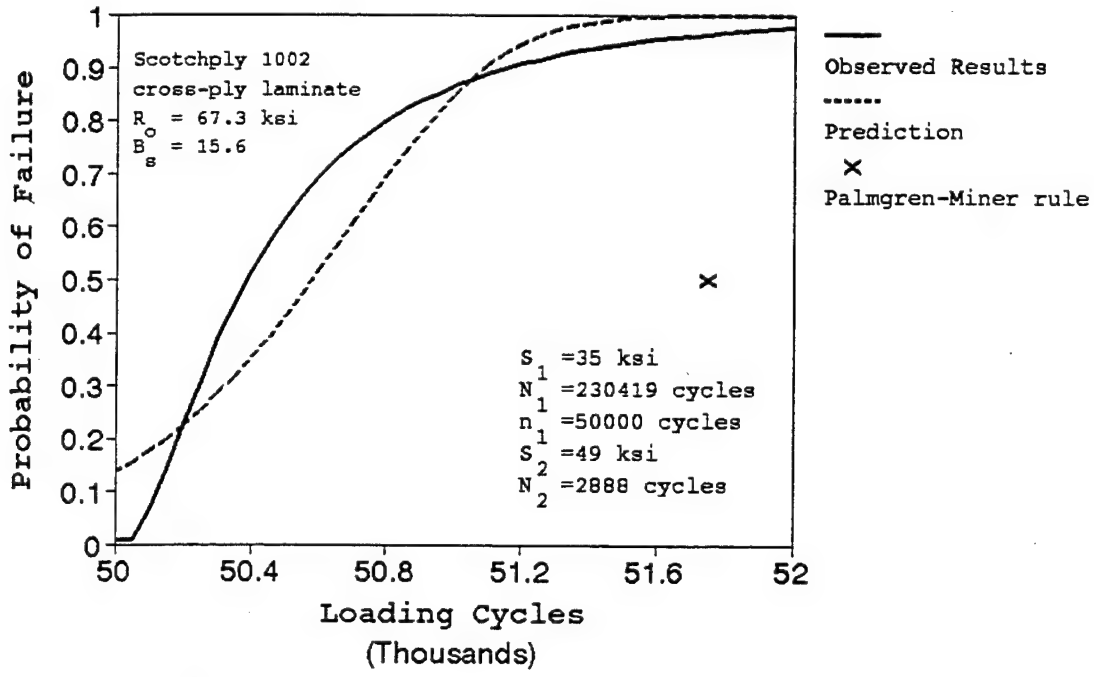

Figure 29. Comparison of predicted and observed results for a low-high large first block loading.

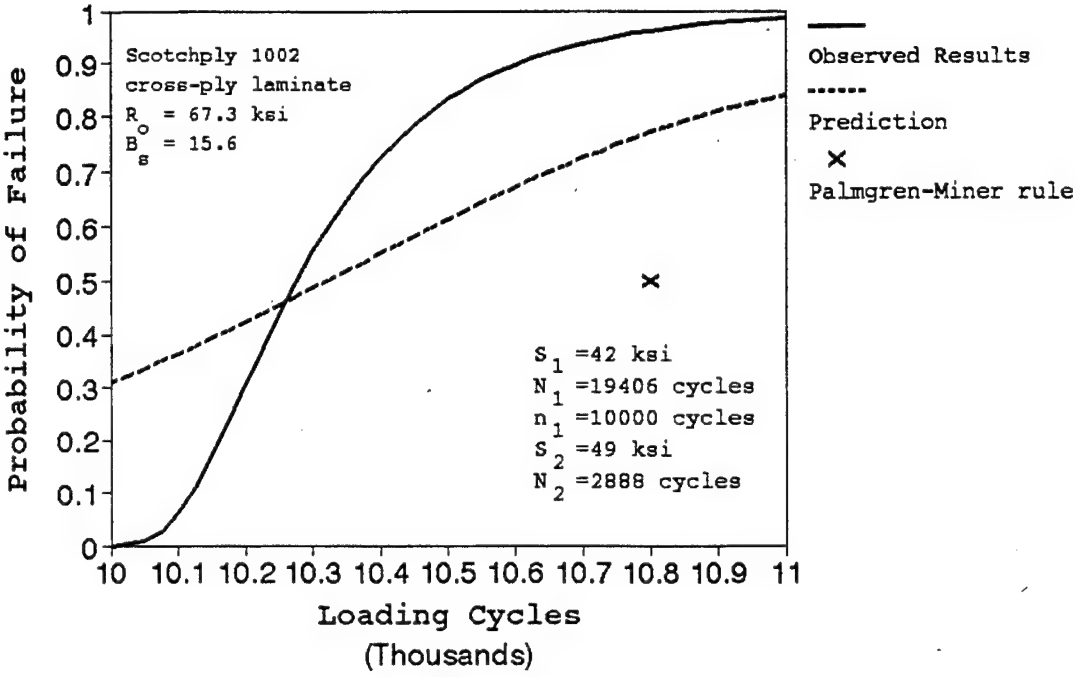

Figure 30. Comparison of predicted and observed results for a low-high large first block loading.

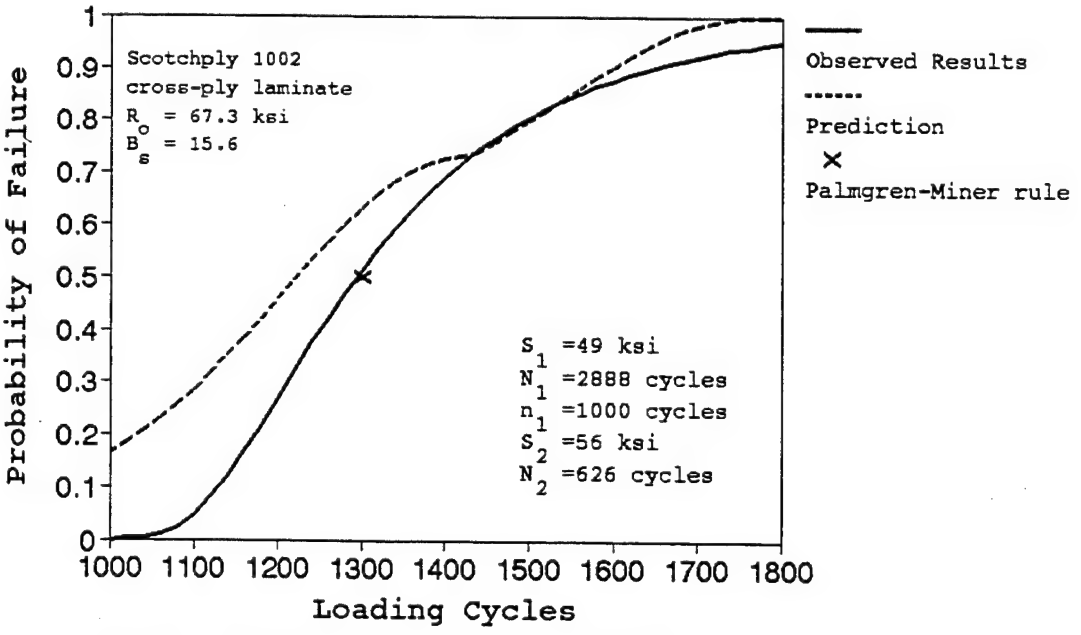

Figure 31. Comparison of predicted and observed results for a low-high large first block loading.

Broutman and Sahu (1972) also presented data from six high-low, large first block loadings, four of which were evaluated by Yang and Jones (1981). The comparison between theory and experiment is presented in Figures 16-21. Of those cases evaluated by Yang and Jones (1981), essentially similar predictive capability is once again observed for the two models; based on Figures 16 and 17, the current model is perhaps slightly better. The worst correlation between predicted and observed results is evidenced in Figures 20 and 21 and occurs for reasons similar to those given above in reference to Figures 14 and 15. As for the small first block loading cases, predictions of mean life by the Palmgren-Miner rule are comparable to those by the wearout models for all loadings.

Figures 22 through 27 compare predicted and observed results for the low-high, small first block loadings. Only the first of these was evaluated by Yang and Jones (1981). For these figures, the number of cycles on the abscissa begins at the second stress level. Yang's probability of failure curve displays good agreement with the experimental fatigue life distribution for the loading of Figure 22. However, based on the single loading case which they evaluated, one cannot substantiate any direct comparisons between models. In general, our model shows reasonable correlation to experiment for all loading cases. In contrast to the high-low results, overall, the Palmgren-Miner rule compared unfavorably to the model's predictions and to experimental results.

Figures 28 through 31 present the predicted and observed results for low-high, large first block loadings; no predictions by Yang and Jones (1981) were presented for these cases. In general, these results are similar to those of the low-high small first block loadings: reasonable predictions are obtained by the model and somewhat worse results (with the exception of Figure 31) are obtained by the Palmgren-Miner rule.

5.2 Cycle Mix Effects

Farrow (1989) evaluated the effect of cycle mix using angle-ply graphite/epoxy laminates subjected to both large and small block two-stress level fatigue loadings. The large block loading was comprised of an initial 100,000 cycles at a maximum stress of 17.66 ksi followed by 1,000 cycles at a maximum stress of 26.66 ksi. This pattern was repeated until the specimen failed. In the small block loading case, the number of cycles at each stress is reduced by a factor of 100. That is, the first sequence consisted of 1,000 cycles at a maximum stress of 17.66 ksi and the second sequence consisted of 10 cycles at 26.66 ksi. The constant amplitude fatigue life data and strength degradation

parameters required to characterize the model for the two-stress levels were obtained from separate constant amplitude fatigue test results and are presented in Table 2. The static strength and shape parameters were found to be R_o=36.4 ksi and B_s=42.9 and were obtained from static strength data reported by Farrow (1989).

Table 2. Wearout Parameters for Constant Amplitude Loading for Angle-ply Laminates

Maximum Stress (ksi)	Minimum Stress (ksi)	Fatigue Life N	B_1	v
26.66	2.67	16351	3.7	2.00
17.66	1.77	1151021	6.0	1.25

Figures 32 and 33 present predicted and observed results for high-low and low-high large block repeating loadings, respectively, and Figure 34 presents results for a low-high small block repeating loading. The experimental results in the figures were obtained from 6 tests and are plotted using Weibull cumulative distributions. Predicted results are presented for our model with the cycle mix factor, CM [cf. Eq.'s (17) and (18)]. Where CM is included, the cycle mix constant, C_m, was obtained by comparing the model predictions to the three sets of data and choosing that value which gave the best correlation. This procedure gave $C_m = 5.38 \times 10^{-7}$. Where CM is not included, we take $C_m = 0$. For clarity, in this latter case only the predicted mean fatigue life is shown in the figures. Predictions are also presented from the Palmgren-Miner rule, and from an interactive parameter cumulative damage (IPCD) model developed by Farrow (1989). The IPCD model predicts mean fatigue life only; it defines damage in terms of the percent change in secant modulus and defines failure when the damage sum equals a value that is empirically related to the static failure strain. Note that essentially no change in the model's predictions are observed for the large block loading cases when the cycle mix factor is included. However, a non-zero value of C_m significantly improves the model's predictions for the small block loading. Also note that the discrepancies between theory and experiment shown in Figures 32 and 33, which are primarily sequencing effects, are overshadowed by the cycle mix effect of Figure 34. This "dominance" of the cycle mix effect will occur for the most practical loadings and, as described earlier, is one reason why we have not concentrated on obtaining better correlation between theory and experiment for two-stress level runout fatigue.

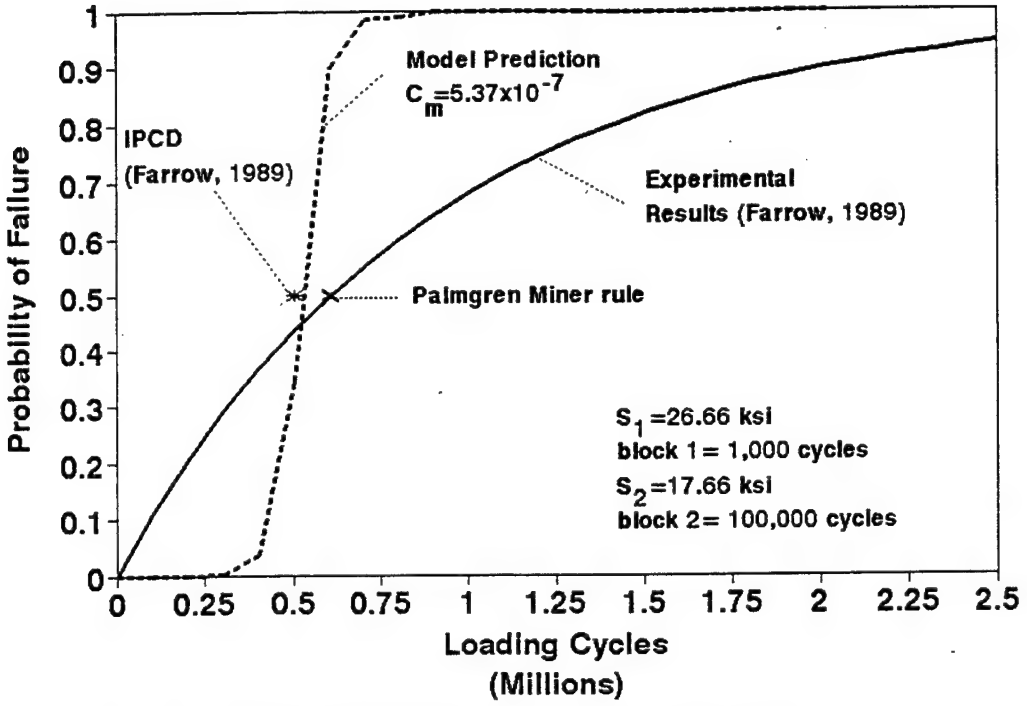

Figure 32. Comparison of predicted and observed results for high-low large block loading on angle-ply graphite/epoxy laminates.

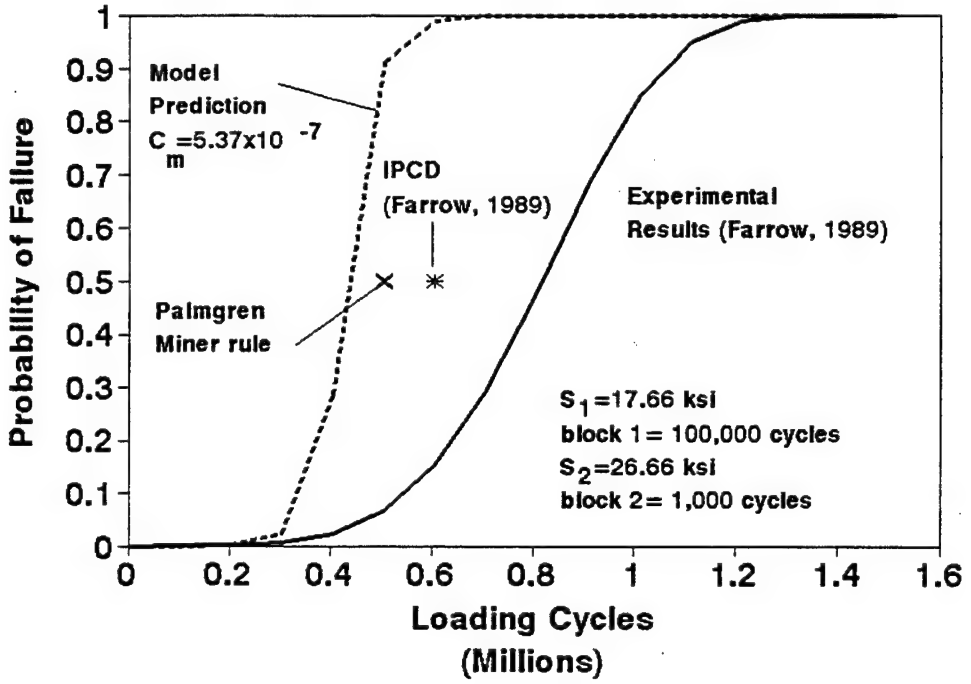

Figure 33. Comparison of predicted and observed results for low-high large block loading on angle-ply graphite/epoxy laminates.

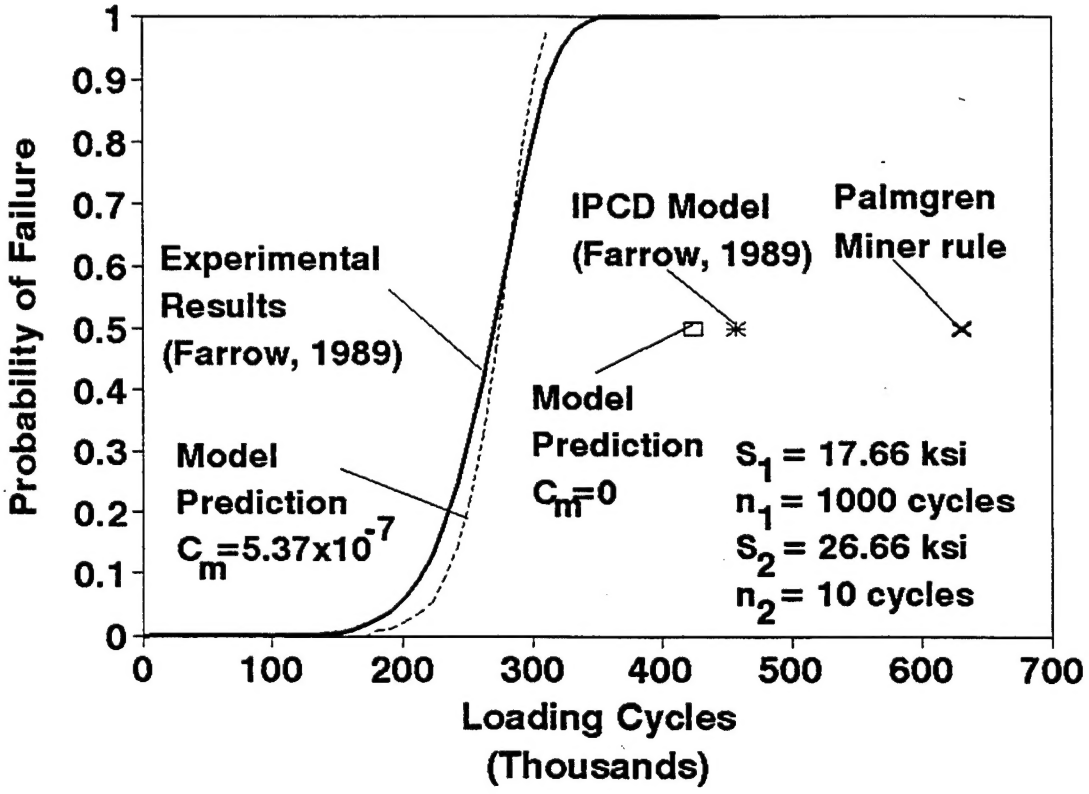

Figure 34. Comparison of predicted and observed results for low-high small block loading of angle-ply graphite/epoxy laminate.

6. CONCLUSION

A strength-based wearout model has been presented for predicting the residual strength and fatigue life of composite laminates subjected to constant amplitude and two-stress level loadings. The model is derived based on three fundamental assumptions: that the laminate or structure of interest is subjected to undergo proportional loading, that strength is a monotonically decreasing function of the number of cycles, and that the probability of failure after an arbitrary number of cycles may be represented by a two parameter Weibull function. The model requires a limited amount of characterization testing to determine the necessary input parameters and this testing must be performed on samples which experience an essentially similar stress state as the structure of interest. By comparison with a large amount of fatigue test data, it has been demonstrated that the model has reasonably good predictive capability, and that this capability equals or exceeds that of other models of which the authors' are aware.

The primary step in extending this model to multi-stress level loading is the development of a procedure for determining all of the model parameters that are required to characterize the stress levels comprising a randomly ordered load spectrum. In Part II of this work (Schaff and Davidson, 1994b), a relatively simple approach is developed. It is shown that only a limited amount of experimental input, primarily from constant amplitude tests at 3 separate stress ratios, is required to fully characterize the model. The model is verified by comparison with experimental results from a number of different laminates and load spectra and good correlation is obtained for all cases.

7. BIBLIOGRAPHY

Broutman, L. J. and Sahu S., 1972, "A New Theory to Predict Cumulative Fatigue Damage in Fiberglass Reinforced Plastics," American Society for Testing and Materials, STP 497, pp. 170-88.

Chou, P. C. and Croman, R., 1978, "Residual Strength in Fatigue Based on the Strength-Life Equal Rank Assumption," Journal of Composite Materials, Vol. 12, pp. 177-95.

Chou, P. C. and Croman, R., 1979, "Degradation and Sudden-Death Models of Fatigue of Graphite/Epoxy Composites," American Society for Testing Materials, STP 674, pp. 431-54.

Farrow, I. R., 1989, "Damage Accumulation and Degradation of Composite Laminates Under Aircraft Service Loading: Assessment and Prediction Vol. I and II," Cranfield Institute of Technology, PhD. Thesis.

Hahn, H.T. and Kim, R. Y., 1975, "Proof Testing of Composite Materials," Journal of Composite Materials, Vol. 9, pp. 297-311.

Hahn, H.T. and Kim, R. Y., 1976, "Fatigue Behavior of Composite Laminates," Journal of Composite Materials, Vol. 10, pp. 156-80.

Halpin, J. C., Johnson, T. A., Waddoups, M. E., 1972, "Kinetic Fracture Models and Structural Reliability," International Journal of Fracture Mechanics, Vol. 8, pp 465-68.

Hwang, W. B. and Han K. S., 1989, "Fatigue of Composite Materials- Damage Model and Life Prediction," Composite Materials: Fatigue and Fracture, 2nd Vol., American Society for Testing and Materials, STP 1012, pp. 87-102.

Hwang, W. and Han, K. S., 1986a, "Fatigue of Composites-Fatigue Modulus Concept and Life Prediction," Journal of Composite Materials, Vol. 20, pp. 154-65.

Hwang, W. and Han, K. S., 1986b, "Cumulative Damage Models and Multi-Stress Fatigue Life Prediction," Journal of Composite Materials, Vol. 20, pp. 125-53.

Kulkarni, S. V., McLaughlin, P., Pipes, R. B., 1976, " Fatigue of Notched Fibre Composite Laminates Part II: Analytical and Experimental Evaluation," NASI-13931.

Lee, L. J., Yang, J. N., and Sheu, D. Y., 1993, "Prediction of Fatigue Life for Matrix-Dominated Composite Laminates," Composite Science and Technology, Vol. 46, pp. 21-28.

McLaughlin, P., Kulkarni, S. V., Huagn, S. N., and Walter, R. B., 1975, "Fatigue of Notched Fibre Composite Laminates Part I: Analytical Model," NASA-CR-132 747.

Miner, M.A., 1945, "Cumulative Damage in Fatigue," Journal of Applied Mechanics, Vol. 12, pp. 159-64.

O'Brien, T. K. and Reifsnider, K. L., 1981, "Fatigue Damage Evaluation Stiffness Measurements in Boron-Epoxy Laminates," Journal of Composite Materials, Vol. 15, pp 55-70.

Palmgren, A., 1924, "Die Lebensdauer von Kugellagern,"Zeitschrift des Vereins Deutscher Ingenieure, Vol. 68, pp. 339-41.

Poursartip, A., Ashby, M. F., and Beaumont, P. W. R., 1986a, " The Fatigue Damage Mechanics of a Carbon Fibre Composite Laminate: I-Development of the Model," Composites Science and Technology, Vol. 25, pp. 193-218.

Poursartip, A. and Beaumont, P. W. R., 1986b, " The Fatigue Damage Mechanics of a Carbon Fibre Composite Laminate: II-Life Prediction," Composites Science and Technology, Vol. 25, pp. 283-99.

Schaff, J. R. and Davidson, B.D., 1994b, "Life Prediction Methodology for Composite Laminates. Part II: Spectrum Fatigue," WL-TR-94-4080, Air Force Wright Laboratory.

Schaff, J. R. and Davidson, B. D., 1994a, "Life Prediction for Composite Laminates Subjected to Spectrum Fatigue Loading," presented during the Durability of Composites Symposium held at 1994 American Society of Mechanical Engineers Winter Annual Meeting, Nov. 8, 1994 in Chicago, IL.

Sendeckyj, G. P., 1990, "Life Prediction for Resin-Matrix Composite Materials," Composite Materials Series: Fatigue of Composites, Vol. 4., pp. 431-83.

Talreja, R., 1985, "Fatigue of Composite Materials," Technical University of Denmark, PhD. Thesis.

Timmer, J. S. and Hahn, H. T., 1993, "The Effect of Preloading on Fatigue Damage in Composites," 18th Annual Mechanics of Composites Review.

Yang, J. N., Yang, S. H., and Jones, D. L., 1989, "A Stiffness-Based Statistical Model for Predicting the Fatigue Life of Composite Laminates," Journal of Composites Technology and Research, Vol. 11, No. 4., pp. 129-34.

Yang, J. N. and Du, S., 1983, "An Exploratory Study Into the Fatigue of Composites Under Spectrum Loading," Journal of Composite Materials, Vol. 17, pp. 511-26.

Yang, J. N. and Jones D. L., 1983, "Load Sequence Effects on Graphite/Epoxy [+-35]2s Laminates," Long-Term Behavior of Composites, American Society for Testing and Materials, STP 813, pp. 246-62.

Yang, J. N. and Jones D. L., 1981, "Load Sequence on the Fatigue of Unnotched Composites Materials," Fatigue of Fiberous Composite Materials, American Society for Testing and Materials, STP 723, pp. 213-32.

Yang, J. N. and Jones D. L., 1980, "Effect of Load Sequence on the Statistical Fatigue of Composites," AIAA Journal, Vol. 12, pp. 1525-31.

Yang, J. N., 1978, "Fatigue and Residual Strength Degradation for Graphite/Epoxy Composites Under Tension-Compression Cyclic Loadings," Journal of Composite Materials, Vol. 12, pp. 19-41.

Yang, J. N. and Liu, M. D., 1977, "Residual Strength Degradation Model and Theory of Periodic Proof Tests for Graphite/Epoxy," Journal of Composite Materials, Vol. 11, pp. 176-203.

Weibull, W., 1967, "Estimation of Distribution Parameters by a Combination of the Best Linear Order Statistics and Maximum Likelihood," AFML-TR-67-105, Air Force Materials Laboratory.

Weibull, W. and Weibull, G.W., 1977, "New Aspects and Methods of Statistical Analysis of Test Data with Spectial Reference to the Normal, the Lognormal, and the Weibull Distributions," FOA Report D 20045-DB, Defense Research Institute, Stockholms.

Whitworth, H. A., 1987, "Modeling Stiffness Reduction of Graphite/Epoxy Composite Laminates," Journal of Composite Materials, Vol. 21, pp. 362-72.

Whitworth, H. A., 1990, "Cumulative Damage in Composites," Journal of Engineering Materials and Technology, Vol. 112, pp. 358-61.